

Spatial causal inference in the presence of unmeasured confounding and interference

Georgia Papadogeorgou* Srijata Samanta†

Abstract

This manuscript bridges the divide between causal inference and spatial statistics, presenting novel insights for causal inference in spatial data analysis, and establishing how tools from spatial statistics can be used to draw causal inferences. We introduce spatial causal graphs to highlight that spatial confounding and interference can be entangled, in that investigating the presence of one can lead to wrongful conclusions in the presence of the other. Moreover, we show that spatial dependence in the exposure variable can render standard analyses invalid, which can lead to erroneous conclusions. To remedy these issues, we propose a Bayesian parametric approach based on tools commonly-used in spatial statistics. This approach simultaneously accounts for interference and mitigates bias resulting from local and neighborhood unmeasured spatial confounding. From a Bayesian perspective, we show that incorporating an exposure model is necessary, and we theoretically prove that all model parameters are identifiable, even in the presence of unmeasured confounding. To illustrate the approach's effectiveness, we provide results from a simulation study and a case study involving the impact of sulfur dioxide emissions from power plants on cardiovascular mortality.

Keywords: Bayesian causal inference; interference; potential outcomes; spatial confounding; spatial causal inference; unmeasured confounding

1 Introduction

Many of the questions researchers are faced with are causal in nature and methodology for drawing causal inferences from observational data has been flourishing. While most methods assume that the sample is randomly chosen from a superpopulation of interest, the reality is often different. In many instances, data exhibits interdependencies which give rise to causal and statistical dependence, and complicate how causal effects are defined and estimated. In this work, we provide an interrogation of the challenges and opportunities in causal inference with spatial data that pertain specifically to the observations' statistical and causal dependence. We simultaneously investigate the implications that arise due to spatial interference, unmeasured spatial confounding, and the variables' inherent spatial

*Department of Statistics, University of Florida, Email: gpapadogeorgou@ufl.edu

†Bristol Myers Squibb

co-dependencies. Our goal is to unite the spatial and causal inference literatures, and address the gaps that arise when a research question is investigated under the lens of one, but not both. On one hand, we draw from the causal inference literature to provide new insights on the complications that arise in the analysis of spatial data. On the other hand, we draw from the spatial statistics literature to develop tools for estimating causal effects from spatial data.

One of the challenges in spatial causal inference pertains to the potential existence of spatial spillover effects: the outcome in one location might be driven by exposures in the same and other locations. This phenomenon is often referred to in the literature as *interference*. When interference is present, the interpretation of estimates from estimators that ignore interference is complicated [Sävje et al., 2021, Tchetgen Tchetgen and VanderWeele, 2012]. Interference has attracted a lot of attention in the last couple of decades [e.g. Sobel, 2006, Hudgens and Halloran, 2008, Manski, 2013, Aronow and Samii, 2017, Tchetgen Tchetgen et al., 2020, Ogburn et al., 2022, among many others] with some studies that focus explicitly on how interference manifests in spatial settings [Verbitsky-Savitz and Raudenbush, 2012, Wang et al., 2020, Zigler et al., 2020, Papadogeorgou et al., 2022, Giffin et al., 2022, Shin et al., 2023, Antonelli and Beck, 2023].

Spatial data also presents opportunities for causal inference that pertain specifically to the data’s spatial dependence structure. The term “spatial confounding” has been used to represent drastically different notions in the spatial and causal literatures [see Reich et al., 2021, Gilbert et al., 2021, Papadogeorgou, 2022, for relevant discussion]. In spatial statistics, it is used to describe collinearity between covariates and spatial random effects in regression models [Reich et al., 2006, Hodges and Reich, 2010, Paciorek, 2010, Hanks et al., 2015, Prates et al., 2019]. Here, we adopt the notion of spatial confounding encountered in causal inference [Papadogeorgou et al., 2019, Gilbert et al., 2021], where the measured variables do not suffice for confounding adjustment, but the missing confounders exhibit a spatial structure. If the unmeasured confounders are spatially varying in that nearby observations have similar values, recent developments harvest this structure to mitigate bias from these unmeasured spatial confounders [Thaden and Kneib, 2018, Papadogeorgou et al., 2019, Keller and Szpiro, 2020, Schnell and Papadogeorgou, 2020, Gilbert et al., 2021, Dupont et al., 2022, Christiansen et al., 2022, Guan et al., 2022]. Therefore, the data’s inherent dependence structure provides an opportunity to mitigate bias due to violations of the no unmeasured confounding assumption in causal inference.

There is very limited literature investigating interference and spatial confounding simultaneously. Graham et al. [2013] adopted a modeling approach which included spatial predictors, spatial random effects, and functions of the neighboring areas’ exposure in a Poisson regression. However, causal quantities of interest are not clearly stated, their approach does not allow for confounding from un-

measured variables, and it is susceptible to biases introduced by spatial random effects. [Giffin et al. \[2021\]](#) investigated an instrumental-variable approach for spatial data, which allowed for the outcome at one location to be driven by the exposure at others. Their approach provides a promising direction forward, though it requires access to a valid instrument.

Our work achieves the following goals. (a) Drawing from established causal inference concepts, we introduce causal diagrams for spatially dependent data. (b) We illustrate theoretically and practically that spatial confounding and spatial spillover effects can manifest as one another: If unmeasured spatial confounding is present and not accounted, investigators might misinterpret the spatial structures induced by the confounder as interference, which would lead to wrongful conclusions about the causal effect of a potential intervention. In reverse, if interference is present and not accounted, researchers might mis-attribute spatial dependencies induced by interference to spatial confounding.

(c) We demonstrate that statistical dependence in the exposure variable can render standard analyses for estimating causal effects invalid. These results indubitably show that establishing causality in spatial settings is faced with unique challenges compared to settings with independent observations. (d) Based on these new causal diagrams for spatial data, we formally establish that neighborhood exposure and confounder values must be incorporated in a spatial causal analysis in order to avoid the aforementioned pitfalls, an important guidance for practitioners. Therefore, the preceding results provide important insights for spatial data analysis when the study's focus is to interpret estimated quantities causally. (e) In the presence of unmeasured spatial confounders, we establish that methodology for causal inference with spatial data should simultaneously account for interference, and local and neighborhood unmeasured confounding. We introduce a Bayesian causal inference framework for spatial data which i) is based on tools amenable to spatial statisticians, ii) incorporates interference, iii) mitigates bias in effect estimation from local and neighborhood unmeasured confounding, iv) provides straightforward uncertainty quantification, and v) establishes that modeling both the exposure and the outcome process is necessary in the presence of unmeasured spatial confounding. (f) We show theoretically that, when dependencies across units form a ring graph, all model parameters are identifiable, even in the presence of interference and unmeasured spatial confounding. (g) Across a variety of dependence structures, we illustrate in simulations that this approach reduces bias in the estimation of local and interference effects that arises due to unmeasured spatial confounding or inherent statistical dependencies. (h) Finally, we analyze county-level data on sulfur dioxide (SO_2) emissions from power plants and cardiovascular mortality. Our approach indicates the presence of some unmeasured spatial confounding that biases effect estimates downwards.

Our primary focus is the intersection of causal inference and spatial data. Although we focus on spatial areal data, the principles we present can be adapted to scenarios involving spatial point-

referenced data or other structural dependencies, and extensions to these scenarios are available with appropriate adjustments. This work contributes to advancing our understanding of causal relationships in spatial contexts, with potential applications in a number of different applied fields where spatial data plays a crucial role.

2 Causal diagrams and identifiability of estimands with paired spatial data

We introduce causal diagrams for spatial data to illustrate that formal causal reasoning is crucial for identifying and addressing the challenges that arise in causal inference with spatial observational data. Causal graphs have been used to establish nonparametric identifiability of causal estimands in a variety of settings [e.g Pearl, 1995, 2000, Avin et al., 2005, Vansteelandt, 2007], and in the presence of interference explicitly [Ogburn and VanderWeele, 2014]. Here, we establish causal diagrams in scenarios where spatial confounding and interference might exist separately or simultaneously, and where the treatment itself exhibits inherent spatial statistical dependence. The results in this section provide insights and guidance for the proper analysis of spatial data when interested in drawing causal inferences.

To establish our key notions and results, we first consider a simplified setting with a binary treatment variable and a population of interest that is a collection of pairs with dependencies within a pair but not across them. Spatial data on an interconnected network, which is our main focus, is discussed in Section 3.

2.1 Causal estimands for paired spatial data with a binary treatment and interference

Consider the situation where there is a natural ordering within pairs of spatial observations that allows us to name them Unit 1 and Unit 2. For example, Unit 1 might be located upstream or upwind of Unit 2. We use i, j to denote the two units, and we drop the notation that corresponds to the pair for simplicity. Consider also a binary treatment that could be applied to or withheld from each of the units. In spatial settings, the treatment applied to one location can often affect the outcome at other locations. The term *spatial interference* is used to represent this situation. In the presence of spatial interference, the units have potential outcomes $Y_i(z_i, z_j)$ and $Y_j(z_j, z_i)$ representing the outcome that would occur for each unit if the pair’s treatment level was set to $z_i, z_j \in \{0, 1\}$. We write the individual’s own treatment first in the notation for potential outcomes. Also, we use λ to denote *local* effects representing the effect on a unit’s outcome for changes in its own treatment, and ι to denote *interference* effects representing the effect on a unit’s outcome for changes in the neighbor’s

treatment. Define the local effect for unit i when fixing the treatment of unit j to z as

$$\lambda_i(z) = \mathbb{E}[Y_i(z_i = 1, z_j = z) - Y_i(z_i = 0, z_j = z)] \equiv \mathbb{E}[Y_i(1, z) - Y_i(0, z)], \quad (1)$$

and the interference effects for unit i when setting its own treatment level at z as

$$\iota_i(z) = \mathbb{E}[Y_i(z_i = z, z_j = 1) - Y_i(z_i = z, z_j = 0)] \equiv \mathbb{E}[Y_i(z, 1) - Y_i(z, 0)], \quad (2)$$

where the expectations are over the pairs. In these definitions, the subscript i represents the unit on whose outcome we focus. Since only one treatment is observed for each unit, only one of the potential outcomes is observed and the remaining are unobserved, often referred to as the fundamental problem of causal inference. Therefore, the causal estimands in (1) and (2) are defined based on unobservable quantities.

Alternative definitions of local and interference effects for stochastic allocations or when the units within a pair are not ordered are given in Supplement A.1. Estimands for blocks of larger or varying sizes are discussed in Supplement A.2. All the results discussed for pairs of units also apply in those cases, so we refrain from discussing them here.

2.2 The observed pair data and causal identifiability

Let $\mathbf{Z} = (Z_1, Z_2)$ and $\mathbf{Y} = (Y_1, Y_2)$ denote the pair-level observed treatment and outcome for the two units. The observed outcomes are equal to the potential outcomes under the observed treatment, $Y_1 = Y_1(Z_1, Z_2)$ and $Y_2 = Y_2(Z_2, Z_1)$. We assume that ignorability holds conditional on a spatial covariate $\mathbf{U} = (U_1, U_2)$. We denote the covariate here with the letter “U” because this covariate will be considered unmeasured later in the manuscript. We refrain from considering additional covariates until Section 3 for ease of exposition.

Assumption 1 (Pair ignorability). It holds that $\mathbf{Z} \perp\!\!\!\perp Y_i(z_1, z_2) \mid \mathbf{U}$ for $i = 1, 2$ and $z_1, z_2 \in \{0, 1\}$. Also, for each $\mathbf{u} = (u_1, u_2)$ such that $P_{\mathbf{U}}(\mathbf{u}) > 0$, we have that $P_{\mathbf{Z}|\mathbf{u}}(\mathbf{z} \mid \mathbf{U} = \mathbf{u}) > 0$, where $\mathbf{z} = (z_1, z_2) \in \{0, 1\}^2$, and $P_{\mathbf{U}}, P_{\mathbf{Z}|\mathbf{u}}$ denote the corresponding distribution across pairs.

It is known that this assumption suffices to establish that the local and interference effects in Section 2.1, which are defined in terms of unobserved potential outcomes, can be written as functions of observable quantities. Crucially, this nonparametric identifiability result establishes that causal effects can be estimated based on data $(\mathbf{U}, \mathbf{Z}, \mathbf{Y})$, where *the pair* is the unit of analysis. Even if such analysis is possible when the population of interest is a collection of pairs, it becomes infeasible when the data arise on an interconnected spatial network as the one in Section 3. Instead, in spatial settings, estimation techniques are at the level of the *unit*, where a unit’s outcome is regressed on their own

treatment and covariates. Therefore, it is crucial that we uncover the complications in identifying causal effects that are not present in cases with independent observations but arise in spatial causal analyses, and provide guidance on how statistical and causal dependencies can be addressed within the context of unit-level analysis.

2.3 Identifiability of estimands in the presence of statistical and causal dependencies

To do so, we introduce expanded causal diagrams for paired spatial data, with the units within a pair depicted separately. We consider cases with spatial confounding, interference, or both, and where the treatment itself exhibits inherent spatial statistical dependence. The interpretation of spatial confounding and inherent dependencies will be discussed below.

We first discuss some basics from causal graph theory. In a causal directed acyclic graph (DAG), nodes represent random variables, and they are connected with arrows. An arrow indicates potential causation from the tail variable to the head variable. No arrow signifies the absence of a causal relationship, but the presence of an arrow doesn't guarantee the occurrence of the depicted relationship. A DAG for the pair spatial data is shown in Figure 1. A backdoor path from Z to Y starts with an arrow pointing into Z and ends with an arrow pointing into Y . If the path is open, conditioning on a variable on this path blocks it, and if all backdoor paths from Z to Y are blocked, the variables are called d-separated, and they are conditionally independent. Colliders are nodes where arrows on either side converge. These nodes block paths when left unconditioned; however, conditioning on a collider opens the path. Since U blocks the backdoor path from Z to Y , the conditional independence statement in Assumption 1 holds.

The graph in Figure 1 compacts the variables at the pair-level which masks the underlying dependencies that are important for investigating identifiability of causal contrasts with unit-level analyses in spatial scenarios. The two units are depicted separately in Figure 2a. The scenarios we consider in this manuscript are depicted in Figure 2b: we do not delve into the situation where the outcome is inherently spatial ($Y_1, \leftrightarrow Y_2$ missing), or the case where U in one location predicts Z in a different location. The double-headed arrows between U_1, U_2 and between Z_1, Z_2 represent *inherent spatial statistical dependencies* due to an underlying common trend that drives both variables. A DAG that represents this structure is shown in Figure 2c: U^u induces correlation between U_1 and U_2 , and similarly for Z^u, Z_1 , and Z_2 . The superscript u is used to stand for *underlying variables* that

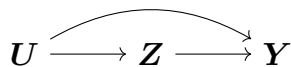
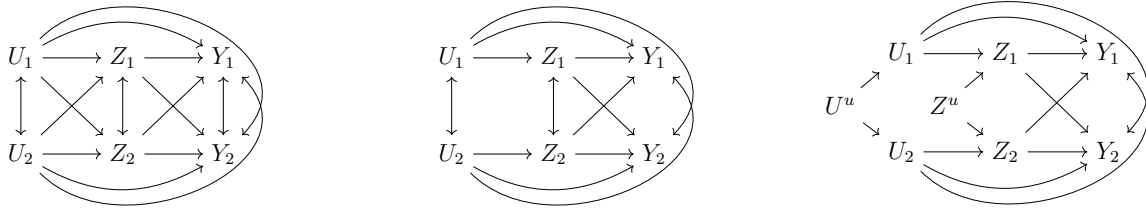


Figure 1: Causal graph at the pair level.



(a) The two units depicted separately with all possible causal and statistical relationships.

(b) The two units with the relationships we consider in this work.

(c) Statistical dependencies occur due to an unobservable underlying common trend.

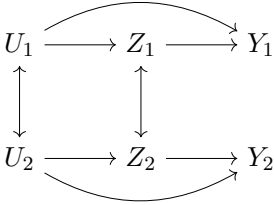
Figure 2: Pair-level causal and statistical dependencies depicted at the unit-level.

drive the spatial structure in the corresponding variable. Such inherent spatial dependence in the treatment variable can occur, for example, by experimental design if different restrictions are applied (or resources are provided) to different geographical areas which would lead to spatially correlated treatment assignments. Inherent spatial structure can also arise by exogenous processes that are possible to measure *in theory* but not in practice, such as the intricate atmospheric and pollution transport processes that dictate the spatially-correlated ambient air pollution levels. Therefore, the underlying U^u and Z^u describe the inherent spatial structure in U and Z which cannot be “adjusted away” by conditioning on more covariates. Finally, the term *spatial confounding* is used to represent the situation where an inherently spatial variable ($U_1 \leftrightarrow U_2$) confounds the relationship of interest, in that it leads to open backdoor paths from the treatment to the outcome.

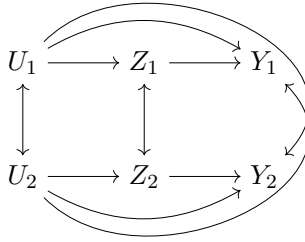
In Figure 3 we present causal diagrams with spatial confounding, interference, and inherent spatial dependence that correspond to subgraphs of Figure 2b with different arrows missing. A researcher that is interested in drawing causal inferences does not know which of these graphs describes the dependencies in their data. We use these graphs to illustrate the complications and biases in estimating causal effects from unit-level analyses that manifest *due to* the spatial dependence in the covariate and the treatment. Conditional independence and identifiability statements are based on viewing the inherent spatial dependencies within the realm of the underlying DAG in Figure 2c. All the identifiability results discussed in this section are stated and proven in Supplement B, some of which are based on well-known theory of graphical models [Spirtes et al., 1993, Pearl, 1995, 2000].

The graphs in Figures 3a and 3b correspond to scenarios with spatial confounding and no interference. Scenario 3a represents the case of *direct* spatial confounding where it is only the *local* value of U that drives the local value for Y . In this scenario there exists *statistical*, but no *causal*, dependence across units. Scenario 3b allows also for *indirect* spatial confounding, which describes a causal dependence across units in that a local spatial predictor of the exposure ($U_j \rightarrow Z_j$) predicts the outcome in a different location ($U_j \rightarrow Y_i$).

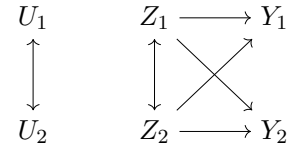
Under scenario 3a, to identify the local causal effects it suffices to control for the local value



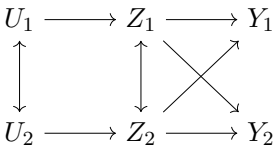
(a) **Direct Spatial Confounding.** The covariate predicts the exposure and the outcome only locally.



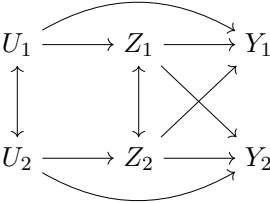
(b) **Direct & Indirect Spatial Confounding.** The covariate predicts the local and neighbor's outcome.



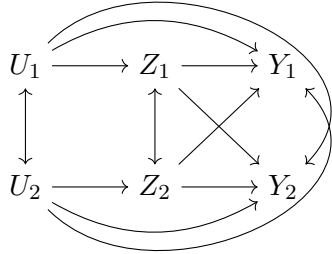
(c) **Spatial interference.** One unit's treatment affects the other unit's outcome. Spatial covariates are not confounders.



(d) **Interference and a spatial predictor of the exposure.**



(e) **Direct Spatial Confounding and Interference.**



(f) **Direct, Indirect Spatial Confounding, and Interference.** The complete graph we consider.

Figure 3: Graphical representation of spatial confounding and interference with a spatially correlated covariate $U = (U_1, U_2)$, a spatial exposure $Z = (Z_1, Z_2)$, and outcome $Y = (Y_1, Y_2)$.

of the confounder. However, there are four backdoor paths for the interference effect of Unit 2's treatment on Unit 1's outcome, $\iota_1(z)$: (A) $Z_2 \leftarrow U_2 \leftrightarrow U_1 \rightarrow Y_1$, (B) $Z_2 \leftarrow U_2 \leftrightarrow U_1 \rightarrow Z_1 \rightarrow Y_1$, (C) $Z_2 \leftrightarrow Z_1 \leftarrow U_1 \rightarrow Y_1$, and (D) $Z_2 \leftrightarrow Z_1 \rightarrow Y_1$. Paths (A) and (B), and paths (C) and (D) exist because U and Z are inherently spatial, respectively. If they were *not* spatial and the two units were independent, the backdoor paths would not exist, and one could identify interference effects without any adjustments. With spatial data, these same analyses would mis-attribute spatial statistical dependence to interference, and mis-identify the presence of spatial interference. Instead, local and interference effects should be investigated simultaneously adjusting for the local value of the confounder. However, in the presence of indirect spatial confounding in Scenario 3b, adjusting for the neighbor's exposure opens the path $Z_i \leftrightarrow Z_j \leftarrow U_j \rightarrow Y_i$ on which Z_j is a collider, and breaks identifiability of the local effect. In this scenario, one needs to adjust for the local *and* the neighbor's confounder value in order to identify local and interference effects. Since this path is only present when Z is spatial, this notion of confounding pertains solely to the setting with dependent data, and it is not met in settings with independent observations.

Figure 3c represents a setting with interference and no spatial confounding. If the exposure Z

is not spatially-structured, the local effect for Unit i can be identified by contrasting the average outcome for this unit among pairs with $Z_i = 1$ and pairs with $Z_i = 0$, without any adjustment. These local effects are different than the ones in Section 2, though they are still interpretable (see Supplement B). However, when Z is inherently spatial, the correlation of Z_1, Z_2 and the interference effect of Z_2 on Y_1 leads to spurious associations for Z_1 and Y_1 , and an estimated quantity that lacks causal interpretation as a local effect. Hence, an analysis that is valid for independent exposures is invalidated for spatially structured exposure variables, even in the complete absence of confounding variables. A similar argument holds for the identification of interference effects for spatial and non-spatial exposures. Therefore, when the exposure is spatial, local and interference effects have to be investigated simultaneously.

In the graph of Figure 3d, the covariate, U , is now a spatial predictor of the exposure but it is not a confounder for the local or the interference effect. For the local effect, there is one additional open backdoor path, $Z_1 \leftarrow U_1 \leftrightarrow U_2 \rightarrow Z_2 \rightarrow Y_1$, compared to the setting in Figure 3c. A researcher might be interested in estimating local effects, while ignoring that interference might be present. Their analysis might adjust for the local variable U , or not. The two analyses will return different values for the local effect estimate, none of which is causally interpretable. Therefore, in this scenario, spatial interference could be mis-interpreted as spatial confounding.

Figure 3e shows a setting with direct spatial confounding and interference, which combines the scenarios in Figures 3a and 3c. When Z is inherently spatial, it is necessary to condition on the local value of the confounder *and* the neighbor's exposure to identify local effects. In contrast, if Z is not inherently spatial, interpretable local effects can be identified conditioning only on the local value of the confounder (see Supplement B). Similar conclusions can be drawn about the identifiability of interference effects. We again see that the exposure's inherent spatial structure can lead to misleading conclusions if not properly accommodated.

Lastly, the graph in Figure 3f represents the situation also shown in Figure 2b with direct spatial confounding, indirect spatial confounding, and interference, of which the other graphs are special cases.

In the presence of interference, it has been previously advocated that neighbors' covariate values have to be adjusted for [Ogburn and VanderWeele, 2014, Forastiere et al., 2021]. However, this previous work does not address non-causal dependencies among observations that might naturally occur in spatial settings. Vansteelandt [2007] considers the setting where treatments within a cluster can be correlated due to unmeasured cluster-level variables, but they do not investigate the role of statistical dependencies in confounders and exposures.

We have addressed both of these points. We have illustrated that adjusting for neighbors' covari-

ate information is particularly important for spatial data analysis. Furthermore, in spatial settings, variables might remain dependent irrespective of how many covariates we condition on. We have established that the variables’ inherent dependence structures lead to challenges in separating statistical dependencies from causal relationships, and accurately attributing causal effects. Our investigations illustrate that spatial settings are intrinsically different from settings with independent observations, in that confounding and causal dependencies can manifest as each other unless the spatial structure of the data is comprehensively accounted for.

These points are illustrated with a motivating simulation study in Supplement C.1, where we illustrate biases of estimators that condition on different sets of variables. We see in practice how researchers might mis-attribute spatial confounding to interference, or mis-identify spatial confounding if interference is not accounted for. We also see that the estimators’ biases increase with the strength of the variables’ spatial dependence. Importantly, across all scenarios, simultaneously estimating local and interference effects while adjusting for local and neighborhood confounder values eliminates biases due to spatial dependencies, an important practical guidance for researchers aiming to draw causal inferences from spatial data.

3 Causal inference with spatial dependencies on a spatial network

In the case of a spatial network of interconnected units, the population of interest cannot be partitioned in non-interacting groups, and defining and estimating causal effects is more challenging. Estimation techniques that consider blocks of interconnected units (such as the pairs of Section 2) as the unit of analysis cannot be applied, and unit-level analyses are the only option. In Section 3.1 we introduce potential outcomes for units across space based on an exposure mapping, in Section 3.2 we introduce ignorability for spatial data with unmeasured confounding, in Section 3.3 we establish estimands based on structural equation modeling, and in Section 3.4 we discuss the interplay between statistical and causal dependence in spatial data.

3.1 Potential outcomes based on network connections and exposure mapping

Let $Z_i \in \mathcal{Z}$ denote the treatment value of unit $i = 1, 2, \dots, n$, which can be binary or continuous. Continuous treatments are often referred to as exposures, so we use the two terms interchangeably. In full generality, a unit’s potential outcomes depend on the treatment level of all units on the spatial network, denoted by $Y_i(\mathbf{z})$ for $\mathbf{z} \in \mathcal{Z}^n$. We reduce the number of potential outcomes by assuming the presence of a known interference network and exposure mapping [Aronow and Samii, 2017, Zigler et al., 2020, Forastiere et al., 2021]. Let A denote a known adjacency matrix of dimension $n \times n$,

where $A_{ij} = 1$ reflects that the outcome for unit i might depend on unit j 's treatment level, $A_{ij} = 0$ otherwise, and all diagonal elements are 0. We assume that unit i 's potential outcomes depend on the treatment vector only through its own exposure, and the average exposure of units with which it is connected through A :

Assumption 2. Let \mathbf{z}, \mathbf{z}' be two treatment vectors in \mathcal{Z}^n such that $z_i = z'_i$ and $\bar{z}_i = \bar{z}'_i$, where $\bar{z}_i = \sum_j A_{ij} z_j / \sum_j A_{ij}$, and similarly for \bar{z}'_i . It holds that $Y_i(\mathbf{z}) = Y_i(\mathbf{z}')$, and the potential outcome $Y_i(\mathbf{z})$ can be denoted as $Y_i(z_i, \bar{z}_i)$.

For areal data, a binary adjacency matrix A often makes sense. However, for the case of point-referenced data the adjacency matrix could be defined as a function of the units' geographical distance with zero-elements on the diagonal. Then, the average neighborhood exposure in Assumption 2 would be a weighted average of the exposures of other locations, with weights driven by the locations' geographic proximity. In settings of spatial interference, exposure mappings have been previously defined based on atmospheric processes in Zigler et al. [2020], and on population mobility in Shin et al. [2023]. Our discussion below would straightforwardly accommodate an asymmetric, weighted adjacency matrix A , or a definition of exposure mapping that is more intricate than the average neighborhood exposure in Assumption 2.

3.2 Ignorability in terms of measured and unmeasured spatial covariates

For identifying and estimating causal effects from observational data, a set of covariates that satisfies ignorability has to be conditioned on. If unconfoundedness is not satisfied based on measured covariates, biases for estimating causal effects persist. For the n units in the network, let $\tilde{C}_i = (C_{i1}, C_{i2}, \dots, C_{ip})^T$ denote unit i 's p measured covariates, which include individual and neighborhood characteristics. However, these covariates are not a sufficient conditioning set for unconfoundedness of the treatment assignment, and

$$(Z_i, \bar{Z}_i) \not\perp\!\!\!\perp Y_i(z, \bar{z}) \mid \tilde{C}_i. \quad (3)$$

We assume however that ignorability holds conditional on measured covariates, and the local and neighborhood value of an unmeasured covariate.

Assumption 3. There exists unmeasured covariate $\mathbf{U} = (U_1, U_2, \dots, U_n)$ such that $(Z_i, \bar{Z}_i) \perp\!\!\!\perp Y_i(z, \bar{z}) \mid \tilde{C}_i, U_i, \bar{U}_i$, for all z, \bar{z} , where \bar{U}_i is the average value of U in the neighborhood of i , $\bar{U}_i = \sum_j A_{ij} U_j / \sum_j A_{ij}$. Also, it holds that $f(Z_i = z, \bar{Z}_i = \bar{z}_i \mid \tilde{C}_i, U_i, \bar{U}_i) > 0$.

Assumption 3 resembles the unconfoundedness assumption on the individual and neighborhood treatment for network data in Forastiere et al. [2021] and Zigler et al. [2020], though here we allow for confounding from local and neighborhood values of an unmeasured covariate.

3.3 Local and interference effects within a structural equation framework

We discuss estimands of interest within the realm of a structural equation model. We assume that for functions f_1, f_2, f_3 , the potential outcomes arise according to

$$Y_i(z, \bar{z}) = f_1(z, \bar{z}) + f_2(\tilde{C}_i) + f_3(U_i, \bar{U}_i) + \epsilon_i(z, \bar{z}) \quad (4)$$

where $\epsilon_i(z, \bar{z})$ are independent mean zero random variables with variance σ_Y^2 . The independence of the error terms across units is a structural representation of the absence of outcome dependence in the graphs of Figure 3 (missing $Y_1 \leftrightarrow Y_2$). For f_1, f_2, f_3 linear, (4) reduces to

$$Y_i(z, \bar{z}) = \beta_0 + \beta_Z z + \beta_{\bar{Z}} \bar{z} + \tilde{C}_i^T \beta_C + \beta_U U_i + \beta_{\bar{U}} \bar{U}_i + \epsilon(z, \bar{z}). \quad (5)$$

Then, β_Z and $\beta_{\bar{Z}}$ describe the local and interference effects of the exposure, respectively, with β_Z representing the expected change in a unit's outcome for a unit increase in its own exposure when the neighborhood exposure remains fixed, and $\beta_{\bar{Z}}$ representing the expected change in a unit's outcome for a unit increase in its neighborhood exposure when its individual exposure remains fixed. Non-linear functions and interaction terms between the local exposure, the neighborhood exposure, and the covariates could be straightforwardly incorporated without any complications.

Structural equation models have been previously employed for defining causal estimands in spatial settings with unmeasured confounders [Schnell and Papadogeorgou, 2020, Christiansen et al., 2022, Papadogeorgou, 2022], interference [Giffin et al., 2022], or both [Giffin et al., 2021], though model-free definitions using potential outcomes directly have also been employed [e.g. Verbitsky-Savitz and Raudenbush, 2012, Gilbert et al., 2021].

The potential outcomes, ignorability assumption, and estimands introduced for data on a spatial network are in-line with the ones for paired data in Section 2. By setting A to be a blocked diagonal matrix with blocks of size two, the potential outcomes $Y_i(z_i, \bar{z}_i)$ reduce to $Y_i(z_i, z_j)$, the ignorability Assumption 3 reduces to the ignorability Assumption 1, and the estimands of interest agree, $\beta_Z = \lambda_i(z)$ and $\beta_{\bar{Z}} = \iota_i(z)$. Therefore, the method in Section 4 applies both to a spatial network and pair data, with the appropriate definition of the adjacency matrix A .

3.4 The bias induced by spatial dependence in network data

We provide an example of how the variables' inherent spatial structure might occur in a spatial setting. This is merely an illustration, and it is not required below. We return to viewing the inherent spatial structure in \mathbf{U} as driven from an underlying covariate U^u as in Figure 2c. For $U^u = (U_1^u, U_2^u, \dots, U_n^u)$ vector of independent random variables, set $U_i = \sum_{j=1}^n w_{ij} U_j^u + \epsilon_i$, for w_{ij} not all zero and ϵ_i independent errors. Then the elements of \mathbf{U} that share elements of U^u are statistically dependent.

If the weights w_{ij} are based on the spatial proximity of i and j , this dependence structure will be *spatially* driven. We can similarly conceive Z^u and Z .

Whether the coefficients in (5) are zero or not can be conceived in the same manner as to whether the corresponding arrows are missing or not in the graphs of Figure 3. Under the different scenarios of Figure 3, the ignorability Assumption 3 might also hold conditional on \tilde{C} only, conditional on \tilde{C} and U , or might only hold conditional on all of \tilde{C} , U and \bar{U} . In Supplement C.2, we investigate the influence of spatial dependencies in learning local and interference effects from a single interconnected network of spatial data. The conclusions are the same as the ones for paired data: (a) spatial confounding and interference can manifest as each other, (b) inherent spatial dependencies complicate standard estimation strategies and can render them invalid even in simple settings, (c) controlling for local and neighborhood covariates is crucial for adjusting for confounding and estimating causal effects unbiasedly, and (d) local and interference effects should be investigated simultaneously in the presence of spatial dependencies.

4 Bayesian inference of local and interference effects with spatial dependencies and unmeasured spatial confounding

Until now we have focused on the complications of identifying causal quantities in spatial settings with confounding, interference, and inherent spatial structure. When the measured covariates do not suffice for confounding adjustment, biases in effect estimation will persist. In what follows, we develop a Bayesian approach for estimating causal effects with spatially dependent data that addresses these complications and mitigates bias due to local and neighborhood unmeasured spatial confounding. In Section 4.1, we show that, in the presence of missing confounders, it is necessary to incorporate the treatment assignment mechanism in a Bayesian causal inference procedure. These derivations inform us of the assumptions on the relationship between the unmeasured confounder and the exposure described in Section 4.2. In Section 4.3, we show theoretically that all model parameters are identifiable from data, even in the presence of unmeasured spatial confounders. In Section 4.4, we design sensible prior distributions for the hyperparameters of the spatial confounder by studying the implications that prior choice on hyperparameters has on the implied prior beliefs of the unmeasured covariate’s confounding strength.

4.1 The role of the treatment assignment mechanism in spatial settings

Bayesian causal inference views unobserved potential outcomes as missing data, and inference on causal effects is acquired from their posterior distribution [Rubin, 1978, Imbens and Rubin, 1997,

Ding and Li, 2018, Li et al., 2022]. Let $\mathbf{Z} = (Z_1, Z_2, \dots, Z_n)$ denote the vector of realized exposures, $\bar{\mathbf{Z}} = (\bar{Z}_1, \bar{Z}_2, \dots, \bar{Z}_n)$ the vector of neighborhood exposures, $\mathbf{C} = (\tilde{C}_1, \tilde{C}_2, \dots, \tilde{C}_n)$ the $n \times p$ matrix of measured covariates, $Y_i(\cdot)$ the collection of all potential outcomes for unit i , and $\mathbf{Y}(\cdot) = \{Y_i(\cdot), \text{ for all } i\}$ the collection of all potential outcomes for all units. Let also $\mathbf{Y}(\cdot) = \{\mathbf{Y}, \mathbf{Y}^{\text{miss}}\}$ where $\mathbf{Y} = (Y_1, Y_2, \dots, Y_n)$ are the observed outcomes and \mathbf{Y}^{miss} is the collection of *unobserved* potential outcomes. Bayesian inference proceeds by specifying $p(\mathbf{Y}(\cdot), \mathbf{Z}, \bar{\mathbf{Z}}, \mathbf{C} \mid \theta)$ and a prior distribution $p(\theta)$, and imputing missing potential outcomes from

$$p(\mathbf{Y}^{\text{miss}} \mid \mathbf{Y}, \mathbf{Z}, \bar{\mathbf{Z}}, \mathbf{C}, \theta) \propto P(\mathbf{Z}, \bar{\mathbf{Z}} \mid \mathbf{Y}(\cdot), \mathbf{C}, \theta) P(\mathbf{Y}(\cdot) \mid \mathbf{C}, \theta) P(\mathbf{C} \mid \theta). \quad (6)$$

If ignorability does not hold based on measured covariates only as in (3), $P(\mathbf{Z}, \bar{\mathbf{Z}} \mid \mathbf{Y}(\cdot), \mathbf{C}, \theta) \neq P(\mathbf{Z}, \bar{\mathbf{Z}} \mid \mathbf{C}, \theta)$. As a result, the treatment assignment mechanism will not “drop out” from (6), and it will be informative for the imputation of missing potential outcomes [McCandless et al., 2007, Ricciardi et al., 2020]. Instead, we write $p(\mathbf{Y}(\cdot), \mathbf{Z}, \bar{\mathbf{Z}}, \mathbf{C})$ as

$$\int p(\mathbf{Y}(\cdot) \mid \mathbf{Z}, \mathbf{C}, \mathbf{U}, \theta^*) p(\mathbf{Z} \mid \mathbf{C}, \mathbf{U}, \theta^*) p(\mathbf{U} \mid \mathbf{C}, \theta^*) p(\mathbf{C} \mid \theta^*) d\mathbf{U} p(\theta^*) d\theta^*$$

where $\bar{\mathbf{Z}}$ is excluded since it is uniquely defined based on \mathbf{Z} , and θ^* extends θ to include parameters governing \mathbf{U} . The structural model (4) implies conditional independence among the outcomes of different units which can only depend on the vector of exposures and the unmeasured covariate through the local and neighborhood values. Therefore,

$$p(\mathbf{Y}(\cdot) \mid \mathbf{Z}, \mathbf{C}, \mathbf{U}, \theta) = \prod_{i=1}^n p(Y_i(\cdot) \mid Z_i, \bar{Z}_i, \tilde{C}_i, U_i, \bar{U}_i, \theta) = \prod_{i=1}^n p(Y_i(\cdot) \mid \tilde{C}_i, U_i, \bar{U}_i, \theta),$$

where the last equality holds from Assumption 3. Hence, we write $p(\mathbf{Y}(\cdot), \mathbf{Z}, \bar{\mathbf{Z}}, \mathbf{C})$ as

$$\int \left[\prod_{i=1}^n p(Y_i(\cdot) \mid \tilde{C}_i, U_i, \bar{U}_i, \theta) \right] p(\mathbf{Z} \mid \mathbf{C}, \mathbf{U}, \theta) p(\mathbf{U} \mid \mathbf{C}, \theta) p(\mathbf{C} \mid \theta) d\mathbf{U} p(\theta) d\theta. \quad (7)$$

Therefore, having access to \mathbf{U} (in addition to \mathbf{C}) would in fact render the treatment assignment ignorable within the Bayesian framework.

These derivations provide interesting insights. Since \mathbf{U} is unknown, and it plays a role in the distribution of the treatment assignment in (7), the treatment assignment has to be incorporated in a valid Bayesian procedure for imputing the missing potential outcomes. This establishes from a new perspective that, within the Bayesian paradigm, simply including a spatial random effect in the outcome model does *not* account for unmeasured spatial confounding since incorporating an exposure model is necessary for proper inference of causal effects.

4.2 Exposure-confounder assumptions

The derivations in (7) also illustrate that it is necessary to specify joint distributions on the unmeasured and measured variables in order to proceed. For continuous exposures, we consider:

Assumption 4. The unmeasured spatial confounder and the spatial exposure have a joint normal distribution conditional on the measured covariates. Specifically,

$$\begin{pmatrix} \mathbf{U} \\ \mathbf{Z} \end{pmatrix} \mid \mathbf{C} \sim N_{2n} \left(\begin{pmatrix} \mathbf{0}_n \\ \gamma_0 \mathbf{1}_n + \mathbf{C}^T \boldsymbol{\gamma}_C \end{pmatrix}, \begin{pmatrix} G & Q \\ Q^\top & H \end{pmatrix}^{-1} \right), \quad (8)$$

for $\boldsymbol{\gamma}_C$ vector of length p , and G, H positive definite matrices. The matrix Q is diagonal with elements $q_i = -\rho\sqrt{g_{ii}h_{ii}}$, where g_{ii}, h_{ii} are the diagonal elements of G, H , respectively.

The joint distribution of \mathbf{U}, \mathbf{Z} is parameterized through its precision matrix. Zero elements of the precision matrix specify conditional independence of the corresponding variables. Therefore, a diagonal Q encodes that $Z_i \perp\!\!\!\perp \mathbf{U}_{-i} \mid U_i, \mathbf{Z}_{-i}, \mathbf{C}$, where $\mathbf{U}_{-i} = (U_1, \dots, U_{i-1}, U_{i+1}, \dots, U_n)$ includes all the entries in \mathbf{U} except the one for unit i , and \mathbf{Z}_{-i} is defined similarly. Under this light, the assumption that Q is diagonal is merely a statistical representation of the absence of an arrow from U_i to Z_j in the graphs of Figures 2 and 3, describing that the unmeasured variable is a driver of only the local exposure level. Even though \mathbf{U} does not depend on \mathbf{C} in Assumption 4, it is reasonable to do so, since the part of the unmeasured variable that is correlated with measured covariates is already adjusted for.

The joint distribution in Assumption 4 has been previously adopted in a related setting [Schnell and Papadogeorgou, 2020]. Our work illustrates two crucial parts with regards to this assumption. We have shown that adopting a joint distribution on (\mathbf{U}, \mathbf{Z}) is necessary within the Bayesian framework (Section 4.1 and equation (7)). Moreover, we have linked the distributional Assumption 4 to the causal relationship of variables viewed through the causal graph representation. Therefore, we provide new insights on the role and interpretation of this assumption through the lens of Bayesian causal inference, and establish how this statistical assumption can be altered based on different assumptions on the complex causal dependence of the two variables.

Since we only have one realization of the spatial exposure \mathbf{Z} , the conditional precision matrices G and H cannot be estimated without imposing some structure on their elements. We assume that G and H are known up to parameter vectors $\theta_U = (\tau_U, \phi_U)$ and $\theta_Z = (\tau_Z, \phi_Z)$, respectively. To ease prior elicitation in Section 4.4 that is consistent for both areal and point-referenced data, we specify $G = \tau_U^2(D - \phi_U A)$ in either case, where D is the diagonal matrix with entries $d_i = \sum_j A_{ij}$. Similarly, we specify $H = \tau_Z^2(D - \phi_Z A)$.

The network’s adjacency matrix is used for defining the neighborhood exposure and covariate in Assumptions 2 and 3, and in the joint precision matrix in Assumption 4. However, these two structures need *not* be the same, and researchers could specify the same or different adjacency matrices for these two components. Furthermore, the functional form with which the exposure is included in the outcome model in (5) can differ from the one in the joint distribution of Assumption 4. Therefore, the framework can easily allow for non-continuous exposures to be considered. We illustrate these points in our data analysis in Section 6.

4.3 Identifiability of model parameters in the presence of unmeasured spatial confounding

It is reasonable to ponder whether the model parameters are identifiable based on the observed data considering they include parameters that correspond to the unmeasured variable and its relationship with the exposure and the outcome.

First, note that the coefficients $\beta_U, \beta_{\bar{U}}$, and the parameter τ_U of the precision matrix G are not identifiable up to scaling of the unmeasured confounder U . To see this, consider $U' = cU$ for some $c \neq 0$. Then, setting $\beta'_{U'} = \beta_U/c$, $\beta'_{\bar{U}} = \beta_{\bar{U}}/c$, and $\tau'^2_{U'} = \tau^2_U/c^2$ will lead to the same value of the likelihood for $(Y, Z, U) \mid C$. Therefore, without loss of generality, we set $\beta_U = 1$. Even though at first sight it might appear that we “force” U in the outcome model by setting $\beta_U = 1$, we show in Section 4.4 that our prior for τ_U ensures that this is not the case.

The next theorem shows that, for a large enough spatial ring network, all model parameters are identifiable, including the causal effects of interest, even in the presence of unmeasured spatial confounding. The definition of a ring graph and the proof are in Supplement D.

Theorem 1. Consider spatial data organized on a ring graph with n nodes. Using data (Z, Y) we can identify whether or not $\rho\phi_U = 0$. If $\rho\phi_U \neq 0$, and for $\beta_U = 1$, we have that all model parameters $(\beta_Z, \beta_{\bar{Z}}, \beta_{\bar{U}}, \rho, \tau_U, \phi_U, \tau_Z, \phi_Z, \sigma_Y^2)$ are identifiable from (Z, Y) as $n \rightarrow \infty$.

If $\rho\phi_U = 0$, there is no spatial predictor of the exposure and therefore no unmeasured spatial confounding. Our proof uses results from Schnell and Papadogeorgou [2020]. However, here, we address complications that arise from the causal cross-dependence of units which impose the inclusion of the neighborhood confounder and exposure values, \bar{U} and \bar{Z} , in the outcome model, along with additional regression coefficients and causal dependence across units. Crucially, Theorem 1 establishes that we can identify complex confounder structures that are not limited to local restrictions.

The proof provides interesting insights for where the information in the data comes from to identify non-local confounding structures. All spatial parameters, $(\tau_U, \phi_U, \tau_Z, \phi_Z)$, and the neighborhood confounding effects, $\beta_{\bar{U}}$, are identified based on the covariance structure in the exposure and the

outcome residuals, and how it attenuates as a function of distance. Interestingly, neighborhood confounding effects are identified by studying the spatial structure in the outcome model residuals that is not explained by similar structure in the exposure model residuals.

Our proof uses the ring graph assumption to acquire a closed form for the data’s covariance matrix. Our conjecture is that identifiability holds for other spatial dependence structures that allow for a sufficient number of location pairs at different distances. This paper does not delve into a comprehensive examination of general identifiability under arbitrary spatial dependence, which is reserved for future research.

4.4 Prior distributions for confounding adjustment

In Bayesian settings, model performance often depends on the choice of hyperparameters, and non-informative priors can lead to poor performance in certain settings [Gelman et al., 2008]. We adopt weakly informative prior distributions for intercepts, coefficients of the measured covariates, and the local and neighborhood exposure and confounder values, the variance of the residual error in (5), and the parameters of the covariance matrix in (8).

We consider measured covariates, exposure and outcome that are standardized to have mean 0 and variance 1. We adopt independent $N(0, \sigma_{\text{prior}}^2)$ prior distributions for the coefficients of all measured covariates, β_C, γ_C and for the intercepts β_0, γ_0 , with $\sigma_{\text{prior}}^2 = 2$. We adopt a $N(0, \sigma_{\text{prior}, \bar{U}}^2)$ prior distribution for $\beta_{\bar{U}}$, and we set $\sigma_{\text{prior}, \bar{U}}^2 = 0.35^2$ to express the prior belief that the importance of the neighborhood value of the confounder is smaller than that of the local value of the confounder (since $\beta_U = 1$). For the residual variance of the outcome model in (5), we specify $\sigma_Y^2 \sim IG(\alpha_Y, \beta_Y)$. We follow a data-driven procedure for choosing the hyperparameters α_Y, β_Y . We regress the outcome on the measured local and neighborhood exposure and the measured covariates and acquire the estimated residual variance, $\tilde{\sigma}_Y^2$. We set $\alpha_Y = 3$ and $\beta_Y = 3 \tilde{\sigma}_Y^2 / 4$, which leads to a prior distribution on the residual variance that puts most of its weight on values smaller than $\tilde{\sigma}_Y^2$, and specifically $P(\sigma_Y^2 < \tilde{\sigma}_Y^2) \approx 0.98$.

Next, we specify prior distributions for the parameters of the joint precision matrix in (8). We specify flat priors for ϕ_Z, ρ on the $(-1, 1)$ interval. We assume that $\phi_U > 0$, and specify $\phi_U \sim \text{Beta}(6, 6)$ to encourage values that imply some spatial dependence (ϕ_U away from 0) while avoiding degenerate distributions (ϕ_U away from 1). We also require that $\phi_Z < \phi_U$ since the exposure should vary within levels of the confounder, in line with conclusions from Paciorek [2010], Schnell and Papadogeorgou [2020] and Dupont et al. [2022].

Lastly, we decide on prior distributions for τ_U, τ_Z . The priors for these parameters can have a large effect on model performance, and their choice requires careful consideration. For simplicity

we discuss in detail the situation where all nodes have the same number of neighbors, and $D = dI_n$ for some $d > 0$ and I_n being the $n \times n$ identity matrix. We can show that $\text{Var}(U_i) \geq (d\tau_U^2)^{-1}$, where equality holds for $\rho = 0$. Since U_i is a priori centered at 0, if the marginal variance of U_i is small for all i , the vector of U is almost indistinguishable from the vector of all zeros, and essentially drops out from the outcome model (even though we set $\beta_U = 1$). Conversely, if the marginal variance of U_i is big a priori, then this prior distribution would imply a strong importance of U in the outcome model (considering $\beta_U = 1$). Therefore, our choice for the prior distribution of the hyperparameter τ_U should be informed by the implied prior distribution on the unmeasured covariate’s confounding strength. We specify a prior distribution for τ_U which avoids the pathological situation that U has an unrealistically high predictive accuracy for the outcome. Specifically, we specify that $1/\tau_U$ has a truncated mean-zero normal distribution with variance $d\sigma_{\text{prior}}^2/2$, and truncated below at 0. The induced prior on $(d\tau_U^2)^{-1}$ ensures that the unmeasured variable’s strength in the outcome model resembles, a priori, the measured covariates’ strength in the outcome model specified by the $N(0, \sigma_{\text{prior}}^2)$ prior distribution on their coefficients.

Similarly, the magnitude of $1/(d\tau_Z^2)$ can be conceived as the variance in the exposure that cannot be explained by covariates. Therefore, $1/\tau_Z^2$ should not be too small because we expect *some* inherent variability in the exposure. At the same time, it should not be too big in comparison to the residual variance of the regression of Z on the measured covariates, denoted by $\tilde{\sigma}_Z^2$. Let \tilde{s}_Z^2 be the observed marginal variance in the exposure across locations. We specify that $1/\tau_Z$ follows a truncated normal distribution centered at $\sqrt{d \tilde{\sigma}_Z^2}/2$ with standard deviation 1, truncated below at $\sqrt{d} 0.01 \tilde{s}_Z^2$ and above at $\sqrt{d \tilde{\sigma}_Z^2}/0.8$.

The prior distributions on τ_U and τ_Z are illustrated in Supplement E. We see that the implied prior distribution on the unmeasured variable’s predictive strength allows for all reasonable values. When the degree is not constant across nodes (which is the case in most networks), we set d to be the median network degree. We sample from the posterior distribution of model parameters using Markov chain Monte Carlo (MCMC). The algorithm is described in Supplement F.

5 Simulations

We perform simulations to evaluate the extent to which the approach introduced in Section 4 mitigates the bias in estimating local and interference causal effects that is caused by direct and indirect unmeasured spatial confounding and the inherent spatial dependence in the exposure. We simulate data under the data generative mechanisms in Figure 3. We consider observations on a network of interconnected units represented by a line graph, where each unit is connected with two others, except for the first and last units which only have one neighbor each. Simulations with pairs of interacting

observations are deferred to Supplement G.

For number of units $n \in \{200, 350, 500\}$, we generated four measured covariates from independent $N(0, 1)$ distributions, the unmeasured confounder and the exposure of interest from (8), and calculated \bar{U}, \bar{Z} for each observation. The outcome was generated according to the linear model in (5) with $\gamma_0 = \beta_0 = 0$. The coefficients of the measured covariates were generated randomly once and were fixed to $\gamma_C = (-0.35, -0.64, 0.49, 0.06)$ and $\beta_C = (0.06, 0.85, 0.02, 0.33)$ throughout our simulations. We specified spatial parameters $\phi_U = 0.6, \phi_Z = 0.4$, and $\rho = 0.35$. For the network data, for which median node degree is equal to 2, we set $\tau_U^2 = \tau_Z^2 = 1$. In all cases, we set the outcome residual error variance to one. The default outcome model coefficients of the local and neighborhood exposure and unmeasured confounder were set to $\beta_Z = 1, \beta_{\bar{Z}} = 0.8, \beta_U = 1$, and $\beta_{\bar{U}} = 0.5$, except for when the relationship does not exist, in which case the corresponding coefficient is set to 0. These specifications match exactly the motivating simulations for the network data discussed in Section 3.4 which are presented in detail in Supplement C.2.

We generate 500 data sets under each of the 36 different scenarios which are combinations of the six scenarios in Figure 3, the three sample sizes, and for network and paired data. We compare the proposed approach to OLS conditional on the measured covariates for estimating local and interference effects. In the absence of unmeasured spatial confounding, the OLS estimator is most efficient for estimating causal effects since it is based on the correctly specified outcome model. Therefore, this comparison informs us of potential efficiency loss when spatial confounding is considered but it is not truly present. In the presence of unmeasured confounding, the OLS estimator incurs confounding bias. Therefore, comparing the two approaches in this setting illuminates the extent to which our approach can alleviate this bias. For our method, we considered two chains with 7,000 iterations as a burn-in period and thinning by 60. We report results for data sets for which the MCMC did not show signs of lack of convergence, evaluated based on the \hat{R} statistic [Vehtari et al., 2021] for β_Z and $\beta_{\bar{Z}}$.

Results for the network data simulations are shown in Table 1. We show bias, root mean squared error (rMSE), and coverage of 95% intervals (confidence intervals for OLS, credible intervals for the Bayesian method). When the unmeasured variable does not confound the relationship of interest (scenarios 3c and 3d) and OLS performs well, our method remains essentially unbiased for both the local and the interference effects. In these settings where our approach is not necessary for controlling for the unmeasured variable, it has slightly larger rMSE than OLS for the local effect, but the two approaches have similar rMSE for estimating the interference effects. These results indicate that the proposed approach might avoid efficiency loss in estimating interference effects when accounting for unmeasured confounding. In all other cases where unmeasured confounding exists (scenarios 3a, 3b, 3e, and 3f), our approach returns significantly lower bias and achieves substantially lower rMSE in

comparison to OLS for all sample sizes, and for both local and interference effects. Furthermore, the proposed approach achieves close to nominal coverage in all scenarios and for both local and interference effects. Our simulations illustrate that our method can protect from biases arising due to unmeasured spatial variables, while ensuring proper inference. Simulations for paired data are shown in Supplement G, and the conclusions are identical.

6 Analyzing environmental health data

To illustrate our method, we investigate the relationship between sulfur dioxide (SO₂) emissions from power plants and cardiovascular health. SO₂ emissions contribute to particulate air pollution which

Table 1: Simulation results with One Interconnected Network. Bias, root mean squared error (rMSE), and coverage of 95% intervals based on OLS and the method of Section 4, for the local and the interference effect. We show simulation results for the 6 settings in Figure 3, and for sample size equal to 200, 350 and 500. Coverage rates are reported as percentages.

True model & sample size	Local effect						Interference effect						
	OLS			Our approach			OLS			Our approach			
	Bias	rMSE	Cover	Bias	rMSE	Cover	Bias	rMSE	Cover	Bias	rMSE	Cover	
$\beta_Z = 0$ and $\beta_{\bar{U}} = 0$													
3a	200	0.492	0.505	0.3	-0.013	0.306	91.6	0.154	0.186	72.3	0.030	0.137	93.4
	350	0.499	0.507	0	-0.060	0.247	94.9	0.146	0.167	55	0.002	0.094	96.6
	500	0.510	0.516	0	-0.073	0.222	96.5	0.157	0.172	36	0.009	0.086	93.8
$\beta_Z = 0$													
3b	200	0.616	0.630	0	-0.169	0.302	96.9	0.277	0.302	34.3	0.027	0.146	93.3
	350	0.624	0.632	0	-0.188	0.283	93.5	0.273	0.288	15	0.004	0.107	95.7
	500	0.639	0.644	0	-0.174	0.253	94.6	0.289	0.299	3.7	0.011	0.092	94.8
$\beta_{UZ} = 0$ and $\beta_U = \beta_{\bar{U}} = 0$													
3c	200	0.003	0.097	95.3	-0.027	0.120	98.8	0.004	0.086	95.7	0.002	0.087	96.2
	350	-0.002	0.072	96	-0.023	0.100	99.7	-0.007	0.066	94.3	-0.016	0.067	95.5
	500	0.001	0.067	92.7	-0.019	0.094	98.7	-0.001	0.056	94	-0.004	0.059	94.1
$\beta_U = 0$ and $\beta_{\bar{U}} = 0$													
3d	200	0.002	0.085	96	-0.020	0.112	99.2	0.003	0.081	96.3	0.004	0.085	95.4
	350	0.000	0.064	95.7	-0.027	0.125	96.7	-0.006	0.063	94	-0.017	0.068	93.9
	500	0.001	0.060	92.7	-0.012	0.113	97.7	-0.001	0.054	94	-0.003	0.056	94.5
$\beta_{\bar{U}} = 0$													
3e	200	0.492	0.505	0.3	0.037	0.296	89.6	0.154	0.186	72.3	0.030	0.141	92
	350	0.499	0.507	0	-0.031	0.234	95.3	0.146	0.167	55	-0.004	0.101	95
	500	0.510	0.516	0	-0.017	0.202	98.6	0.157	0.172	36	0.011	0.088	92.9
3f	200	0.616	0.630	0	-0.139	0.279	97.1	0.277	0.302	34.3	0.019	0.145	94.2
	350	0.624	0.632	0	-0.155	0.254	93.9	0.273	0.288	15	0.000	0.106	95.7
	500	0.639	0.644	0	-0.144	0.229	95	0.289	0.299	3.7	0.008	0.091	95

has been linked to a number of adverse health outcomes [Dominici et al., 2014]. Emissions from one location can potentially affect the outcomes in other locations [Henneman et al., 2019, Zigler and Papadogeorgou, 2021]. We investigate the relationship between local and neighborhood SO₂ emissions from power plants on cardiovascular mortality among the elderly (65 years old or older) at the county level while addressing potentially missing spatial confounders. For a county, neighborhood SO₂ emissions are defined using a 2nd degree adjacency matrix: the total SO₂ emissions from neighboring and neighbors of neighboring counties. A description of data compilation and visualizations are included in Supplement H. Our data includes all the counties (445) in the continental US with local and neighborhood SO₂ emissions.

We analyzed the data using OLS (which ignores potential unmeasured spatial confounding) and our approach. We considered a number of different analyses that illustrate a researcher’s options for analyzing spatial data using our method. We considered analyses that include the exposure variable linearly or logarithmically in the outcome model. Since the exposure is included as is in the joint distribution of (8), using the logarithmic transformation of the exposure in the outcome model illustrates that different functions of the exposure can be specified in different parts of the model. Furthermore, we considered our approach based on a 1st degree, or a 2nd degree adjacency matrix for the spatial relationship of variables in (8). Since the neighborhood exposure is defined based on a 2nd degree adjacency matrix, using a 1st degree adjacency matrix for the precision matrix illustrates that a researcher can use different neighborhood structures for different aspects of the analysis. Lastly, in terms of measured covariates, we adjusted for power plant covariates only, or power plant and demographic covariates. In both cases, local and neighborhood measured covariate levels were included in the model.

The results are shown in Figure 4 as the estimated change in the number of deaths per 100,000 residents for a one standard deviation increase in the local or neighborhood exposure. The estimates from all analyses are comparable. Our approach almost always returns effect estimates that are more positive, towards the expected relationship between SO₂ emissions and cardiovascular mortality, illustrating that there is potential spatial confounding with a 1st or 2nd degree spatial structure. Our approach using a linear function of the exposure in the outcome model and a 2nd degree adjacency matrix for the unmeasured spatial confounder returns statistically significant effect estimates for the interference effect, with 51.9 (95% CI: 3.3 to 101.1) deaths caused for a one standard deviation increase in the neighborhood SO₂ emissions. OLS analyses including weather variables returned similar estimates (see Supplement H).

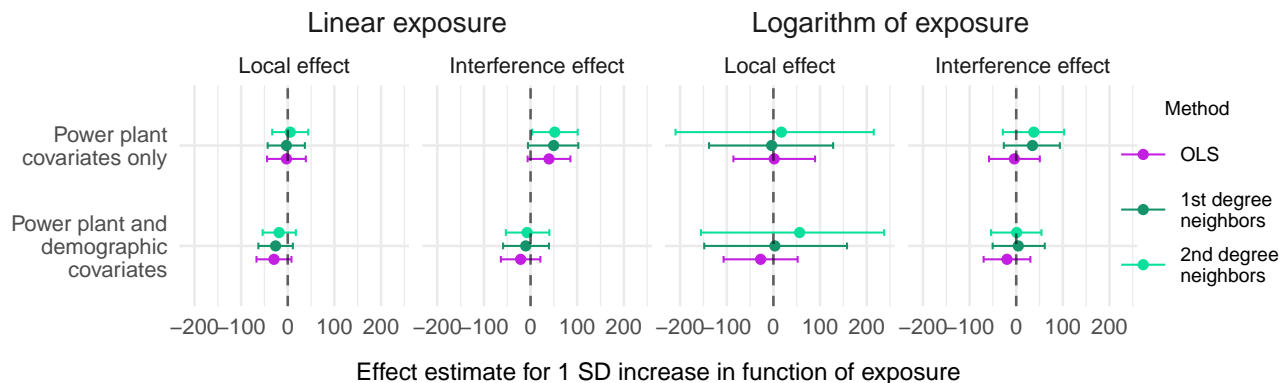


Figure 4: Local and neighborhood effect estimates from OLS and the proposed approach based on 1st or 2nd degree neighbor specification for the spatial variables. The exposure is included in the outcome model linearly (left two panels) or logarithmically (right two panels). Estimates and 95% intervals correspond to the maximum likelihood estimates and confidence interval for OLS, and the posterior mean and credible interval for our approach.

7 Discussion

In this manuscript we discussed the inherent challenges and opportunities that arise in causal inference with spatial data. We illustrated the complications that arise from the data’s inherent dependence structure, and discussed the interplay of spatial confounding and interference. Unmeasured spatial confounding does not necessarily have to exist due to a completely missed covariate. Instead, it is possible that a confounder is mis-measured, or its functional form not correctly included in the outcome model. In these settings, employing a procedure that mitigates bias from unmeasured spatial covariates can improve estimation and inference.

Despite the potential merits of this work, important open questions remain in order to better understand causality in dependent settings. In all scenarios we considered here, we assumed that the outcome is not inherently spatial, though it might exhibit spatial dependence when its spatial predictors are not conditioned on. We suspect that an inherently spatial outcome variable will create additional complications in defining and estimating local and interference effects. We believe that our advancements in drawing causal graphs in spatial settings in Section 2 and interpreting the spatial dependencies as a common underlying spatial trend in Figure 2c can provide a way forward in this setting. It is worth noting here that an inherently dependent outcome variable is entirely different from outcome dependencies that occur through contagion, and the interplay of the two in estimating causal effects is an interesting question for future research.

Acknowledgements

This material is based on work supported by the National Science Foundation under Grant No 2124124.

References

- Joseph Antonelli and Brenden Beck. Heterogeneous causal effects of neighbourhood policing in New York City with staggered adoption of the policy. *Journal of the Royal Statistical Society Series A: Statistics in Society*, 186(4):772–787, 04 2023.
- Peter M Aronow and Cyrus Samii. Estimating average causal effects under general interference, with application to a social network experiment. *Annals of Applied Statistics*, 11(4):1912–1947, 2017.
- Chen Avin, Ilya Shpitser, and Judea Pearl. Identifiability of path-specific effects. *Proceedings of the International Joint Conference on Artificial Intelligence*, pages 357–363, 2005.
- Rune Christiansen, Matthias Baumann, Tobias Kuemmerle, Miguel D Mahecha, and Jonas Peters. Toward causal inference for spatio-temporal data: conflict and forest loss in colombia. *Journal of the American Statistical Association*, 117(538):591–601, 2022.
- Peng Ding and Fan Li. Causal inference: A missing data perspective. *Statistical Science*, 33(2): 214–237, 2018.
- Francesca Dominici, Michael Greenstone, and Cass R Sunstein. Particulate matter matters. *Science*, 344(6181):257–259, 2014.
- Emiko Dupont, Simon N Wood, and Nicole H Augustin. Spatial+: a novel approach to spatial confounding. *Biometrics*, 78(4):1279–1290, 2022.
- Laura Forastiere, Edoardo M Airoidi, and Fabrizia Mealli. Identification and estimation of treatment and interference effects in observational studies on networks. *Journal of the American Statistical Association*, 116(534):901–918, 2021.
- Andrew Gelman, Aleks Jakulin, Maria Grazia Pittau, and Yu-Sung Su. A weakly informative default prior distribution for logistic and other regression models. *The Annals of Applied Statistics*, 2: 1360–1383, 2008.

- Andrew Giffin, Brian J Reich, Shu Yang, and Ana G Rappold. Instrumental variables, spatial confounding and interference. *arXiv preprint arXiv:2103.00304*, 2021.
- Andrew Giffin, BJ Reich, Shu Yang, and AG Rappold. Generalized propensity score approach to causal inference with spatial interference. *Biometrics*, 2022.
- Brian Gilbert, Abhirup Datta, Joan A Casey, and Elizabeth L Ogburn. A causal inference framework for spatial confounding. *arXiv preprint arXiv:2112.14946*, 2021.
- Daniel J Graham, Emma J McCoy, and David A Stephens. Quantifying the effect of area deprivation on child pedestrian casualties by using longitudinal mixed models to adjust for confounding, interference and spatial dependence. *Journal of the Royal Statistical Society: Series A (Statistics in Society)*, 176(4):931–950, 2013.
- Yawen Guan, Garritt L Page, Brian J Reich, Massimo Ventrucchi, and Shu Yang. A spectral adjustment for spatial confounding. *Biometrika*, 2022.
- Ephraim M. Hanks, Erin M. Schliep, Mevin B. Hooten, and Jennifer A. Hoeting. Restricted spatial regression in practice: Geostatistical models, confounding, and robustness under model misspecification. *Environmetrics*, 26(4):243–254, 2015. ISSN 1099095X.
- Lucas RF Henneman, Christine Choirat, and Corwin M Zigler. Accountability assessment of health improvements in the united states associated with reduced coal emissions between 2005 and 2012. *Epidemiology (Cambridge, Mass.)*, 30(4):477, 2019.
- James S Hodges and Brian J Reich. Adding Spatially-Correlated Errors Can Mess Up the Fixed Effect You Love. *The American Statistician*, 64(4):325–334, 2010.
- Michael G Hudgens and M. Elizabeth Halloran. Toward Causal Inference With Interference. *Journal of the American Statistical Association*, 103(482):832–842, jun 2008.
- Guido W Imbens and Donald B Rubin. Bayesian inference for causal effects in randomized experiments with noncompliance. *The annals of statistics*, pages 305–327, 1997.
- Joshua P Keller and Adam A Szpiro. Selecting a scale for spatial confounding adjustment. *Journal of the Royal Statistical Society. Series A,(Statistics in Society)*, 183(3):1121, 2020.
- Fan Li, Peng Ding, and Fabrizia Mealli. Bayesian causal inference: A critical review. *arXiv preprint arXiv:2206.15460*, 2022.

- Charles F Manski. Identification of treatment response with social interactions. *The Econometrics Journal*, 16(1):S1–S23, 2013.
- Lawrence C McCandless, Paul Gustafson, and Adrian Levy. Bayesian sensitivity analysis for unmeasured confounding in observational studies. *Statistics in medicine*, 26(11):2331–2347, 2007.
- Elizabeth L Ogburn and Tyler J VanderWeele. Causal diagrams for interference. *Statistical Science*, pages 559–578, 2014.
- Elizabeth L Ogburn, Oleg Sofrygin, Ivan Diaz, and Mark J Van der Laan. Causal inference for social network data. *Journal of the American Statistical Association*, pages 1–15, 2022.
- Christopher J Paciorek. The importance of scale for spatial-confounding bias and precision of spatial regression estimators. *Statistical Science*, 25(1):107–125, 2010.
- Georgia Papadogeorgou. Discussion on “spatial+: a novel approach to spatial confounding” by emiko dupont, simon n. wood, and nicole h. augustin. *Biometrics*, 78(4):1305–1308, 2022.
- Georgia Papadogeorgou, Christine Choirat, and Corwin M Zigler. Adjusting for unmeasured spatial confounding with distance adjusted propensity score matching. *Biostatistics*, 20(2):256–272, 2019.
- Georgia Papadogeorgou, Kosuke Imai, Jason Lyall, Fan Li, et al. Causal inference with spatio-temporal data: Estimating the effects of airstrikes on insurgent violence in iraq. *Journal of the Royal Statistical Society Series B*, 84(5):1969–1999, 2022.
- Judea Pearl. Causal diagrams for empirical research. *Biometrika*, 82(4):669–688, 1995.
- Judea Pearl. Models, reasoning and inference. *Cambridge, UK: Cambridge University Press*, 19(2), 2000.
- Marcos Oliveira Prates, Renato Martins Assunção, and Erica Castilho Rodrigues. Alleviating Spatial Confounding for Areal Data Problems by Displacing the Geographical Centroids. *Bayesian Analysis*, 14(2):623 – 647, 2019.
- Brian J Reich, James S Hodges, and Vesna Zadnik. Effects of residual smoothing on the posterior of the fixed effects in disease-mapping models. *Biometrics*, 62(4):1197–1206, 2006.
- Brian J Reich, Shu Yang, Yawen Guan, Andrew B Giffin, Matthew J Miller, and Ana Rappold. A review of spatial causal inference methods for environmental and epidemiological applications. *International Statistical Review*, 89(3):605–634, 2021.

- Federico Ricciardi, Alessandra Mattei, and Fabrizia Mealli. Bayesian inference for sequential treatments under latent sequential ignorability. *Journal of the American Statistical Association*, 115(531):1498–1517, 2020.
- Donald B Rubin. Bayesian inference for causal effects: The role of randomization. *The Annals of statistics*, pages 34–58, 1978.
- Fredrik Sävje, Peter Aronow, and Michael Hudgens. Average treatment effects in the presence of unknown interference. *Annals of statistics*, 49(2):673, 2021.
- Patrick M Schnell and Georgia Papadogeorgou. Mitigating unobserved spatial confounding when estimating the effect of supermarket access on cardiovascular disease deaths. *The Annals of Applied Statistics*, 14(4):2069–2095, 2020.
- Heejun Shin, Danielle Braun, Kezia Irene, and Joseph Antonelli. A spatial interference approach to account for mobility in air pollution studies with multivariate continuous treatments. *arXiv preprint arXiv:2305.14194*, 2023.
- Michael E Sobel. What Do Randomized Studies of Housing Mobility Demonstrate? *Journal of the American Statistical Association*, 101(476):1398–1407, 2006.
- Peter Spirtes, Clark N Glymour, Richard Scheines, and David Heckerman. *Causation, prediction, and search*. New York: Springer, 1993.
- E. J. Tchetgen Tchetgen and T. J. VanderWeele. On causal inference in the presence of interference. *Statistical Methods in Medical Research*, 21(1):55–75, 2012.
- Eric J. Tchetgen Tchetgen, Isabel R. Fulcher, and Ilya Shpitser. Auto-G-Computation of Causal Effects on a Network. *Journal of the American Statistical Association*, 2020. ISSN 23318422.
- Hauke Thaden and Thomas Kneib. Structural equation models for dealing with spatial confounding. *The American Statistician*, 72(3):239–252, 2018.
- Stijn Vansteelandt. On confounding, prediction and efficiency in the analysis of longitudinal and cross-sectional clustered data. *Scandinavian journal of statistics*, 34(3):478–498, 2007.
- Aki Vehtari, Andrew Gelman, Daniel Simpson, Bob Carpenter, and Paul-Christian Bürkner. Rank-normalization, folding, and localization: An improved \hat{r} to assess convergence of mcmc (with discussion). *Bayesian analysis*, 16(2):667–718, 2021.

Natalya Verbitsky-Savitz and Stephen W Raudenbush. Causal Inference Under Interference in Spatial Settings : A Case Study Evaluating Community Policing Program in Chicago. *Epidemiologic Methods*, 1(1):105–130, 2012. ISSN 2161-962X.

Ye Wang, Cyrus Samii, Haoge Chang, and PM Aronow. Design-based inference for spatial experiments with interference. *arXiv preprint arXiv:2010.13599*, 2020.

Corwin Zigler, Vera Liu, Laura Forastiere, and Fabrizia Mealli. Bipartite interference and air pollution transport: Estimating health effects of power plant interventions. *arXiv preprint arXiv:2012.04831*, 2020.

Corwin M. Zigler and Georgia Papadogeorgou. Bipartite Causal Inference with Interference. *Statistical Science*, 36(1):109–123, 2021. ISSN 21688745.

Supplementary Materials for:
 Spatial causal inference in the presence of unmeasured confounding
 and interference

Georgia Papadogeorgou, Srijata Samanta

Table of Contents

A Causal estimands for a population of blocks	3
A.1 Alternative definitions of local and interference effects with paired data	3
A.2 Blocked interference with more than two units	3
B Identifiability of quantities under different graphs	3
B.1 Graph 3a: Direct spatial confounding	4
B.2 Graph 3b: Direct and indirect spatial confounding	5
B.3 Graph 3c: Spatial interference	6
B.4 Graph 3d: Interference with spatial predictor of the exposure	8
B.5 Graph 3e: Direct spatial confounding and interference	10
C Motivating simulation studies	12
C.1 Motivating simulation study with paired data	12
C.2 Motivating simulation study in a setting with one spatial network of observations .	13
D Identifiability of model parameters	15
E Illustration of prior distributions	21
E.1 Prior distribution for τ_U	21
E.2 Prior distribution for τ_Z	23

E.3	Implied prior distributions when $\rho \neq 0$	23
F	Posterior distribution sampling scheme	26
G	Simulation results on pairs of data	28
H	Additional study information	30
H.1	The data set	30
H.2	Analysis including weather variables	31

Supplement A. Causal estimands for a population of blocks

A.1 Alternative definitions of local and interference effects with paired data

Alternate definitions of local effects draw the treatments for other units from a pre-specified distribution. For $\pi \in [0, 1]$, we use $\lambda_i(\pi)$ to denote the local effect for unit i when the treatment of unit j is drawn from a Bernoulli distribution with probability π , and $\lambda_i(\pi) = \pi\lambda_i(1) + (1 - \pi)\lambda_i(0)$. Similarly, the interference effect of unit i when their own treatment is drawn from a Bernoulli(π) distribution is denoted by $\iota_i(\pi)$ and $\iota_i(\pi) = \pi\iota_i(1) + (1 - \pi)\iota_i(0)$. For $\pi \in \{0, 1\}$ these definitions revert back those in (1) and (2). If there does not exist a natural ordering of the units within a pair, then the local and interference causal effects could be defined as $\lambda(z) = (\lambda_1(z) + \lambda_2(z))/2$, and $\iota(z) = (\iota_1(z) + \iota_2(z))/2$, respectively, for $z \in \{0, 1\}$.

A.2 Blocked interference with more than two units

For interference blocks that are larger than two units, estimands for local and interference effects can be defined to average over hypothetical distributions of the neighbors' treatments, in agreement to literature on partial interference [Hudgens and Halloran, 2008, Tchetgen Tchetgen and VanderWeele, 2012]. We define the average outcome for unit i when its treatment is set to a fixed value $z \in \{0, 1\}$, and the treatment of the other units in the block, \mathbf{z}_{-i} , are independent draws from a Bernoulli distribution with probability of success $\pi \in [0, 1]$ as $\bar{Y}_i(z, \pi) = \sum_{\mathbf{z}_{-i}} Y_i(z_i = z, \mathbf{z}_{-i})p(\mathbf{z}_{-i}; \pi)$, where $p(\cdot; \pi)$ is the joint probability mass function for independent Bernoulli trials with probability of success π . Then, the local effect for unit i can be defined as $\lambda_i(\pi) = \mathbb{E} [\bar{Y}_i(1, \pi) - \bar{Y}_i(0, \pi)]$, and the interference effect on unit i as $\iota_i(\pi, \pi'; z) = \mathbb{E} [\bar{Y}_i(z, \pi') - \bar{Y}_i(z, \pi)]$. For $\pi, \pi' \in \{0, 1\}$ and for blocks with two units, these estimands revert back to the estimands in (1) and (2), respectively.

Spatial dependence in confounders and exposure values will lead to the same complications in identifying local and interference effects discussed for paired data. To avoid distraction, we do not delve into blocked data with more than two units further. Instead, in Section 3 we focus on data on a single spatial network.

Supplement B. Identifiability of quantities under different graphs

Here, we state and prove all identifiability (and lack of) results stated in Section 2. For identifiability, we view the dependencies in Figure 3 in terms of the underlying spatial structure shown in Figure 2c. Many of these statements have proofs that are straightforward based on the existing theory

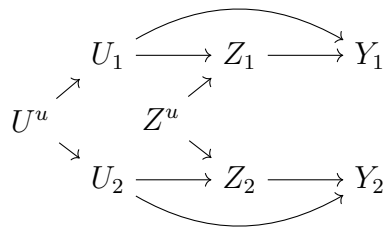
on graphical models [Spirtes et al., 1993, Pearl, 1995, 2000], but we include them here for completeness. Furthermore, we prove any statements about identifiability of local and interference effects that are less obvious because they pertain specifically to the spatial structure of the observations or the presence of spatial interference.

B.1 Graph 3a: Direct spatial confounding

Proposition S.1 (Identifiability of local and interference effects under direct spatial confounding). For variables with causal relationships depicted in Figure 3a, the following statements hold:

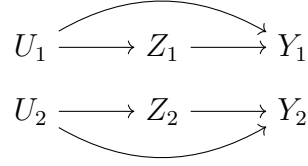
1. Local effects can be identified by controlling for local confounder.
2. If U, Z are not spatial, interference effects can be identified without any adjustment.
3. If U, Z are spatial, interference effects can be identified by controlling for the local value of the exposure and the confounder.

Proof of Proposition S.1. The dependencies in this scenario are depicted in the following graph, where we include the underlying U^u, Z^u that drive the covariate's and the exposure's spatial dependence:



We use the theory on identifiability based on graphical models. We investigate the presence of backdoor paths from the local or neighborhood exposure on the outcome for local and interference effects, respectively. In this setting, interference effects are non-existent and $t_i(z) = 0$.

1. Since this is a scenario without interference, potential outcomes can be denoted as $Y_i(z_i, z_j) = Y_i(z_i)$. Therefore, it suffices to study backdoor paths from Z_i to Y_i . The only such backdoor path is $Z_i \leftarrow U_i \rightarrow Y_i$. Therefore, controlling for the local value of the confounder, U_i , blocks this path, and local effects for Unit i are identified.
2. If U, Z are not spatial, the causal graph is of the form:



and clearly Z_2 and Y_1 are (unconditionally) independent. Therefore the interference effect on Unit 1 is identified as a contrast of Unit 1 outcomes between pairs that have $Z_2 = 1$ and pairs that have $Z_2 = 0$, since

$$\iota_1(z) = 0 = \mathbb{E}[Y_1 \mid Z_2 = 1] - \mathbb{E}[Y_1 \mid Z_2 = 0].$$

3. If U, Z are spatial, Z_2 and Y_1 are not (unconditionally) independent, and therefore we expect that $\mathbb{E}[Y_1 \mid Z_2 = 1] - \mathbb{E}[Y_1 \mid Z_2 = 0] \neq 0$, which means that it does not identify $\iota_1(z)$.

Here, all backdoor paths from Z to Y_1 are blocked by U_1 . Therefore, interference effects can be identified by controlling for the local value of the exposure and the confounder as

$$\iota_1(z) = \mathbb{E} [\mathbb{E}(Y_1 \mid Z_1 = z, U_1, Z_2 = 1) - \mathbb{E}(Y_1 \mid Z_1 = z, U_1, Z_2 = 0)],$$

where the outer expectation is with respect to U_1 .

□

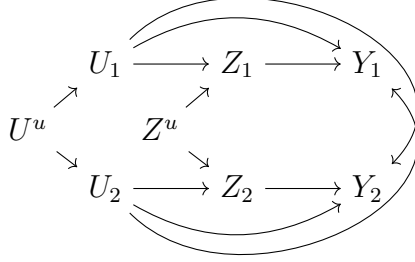
B.2 Graph 3b: Direct and indirect spatial confounding

Proposition S.2 (Identifiability of local and interference effects under direct and indirect spatial confounding). For variables with causal relationships depicted in Figure 3b, the following statements hold:

1. Local and interference effects can be identified by controlling for the local and neighborhood covariate value.
2. When the exposure is inherently spatial, controlling for the neighborhood exposure and the local covariate does not suffice to identify local effects.

Proof of Proposition S.2. We again focus on local and interference effects for Unit 1. Results for the effects on Unit 2 are identical.

1. The graph describing this setting is depicted below:



The vector \mathbf{U} blocks all backdoor paths from the vector \mathbf{Z} to the outcome unit 1, Y_1 , and therefore it holds that $\mathbf{Z} \perp\!\!\!\perp Y_1(z_1, z_2) \mid \mathbf{U}$. This implies that

$$\mathbb{E}[Y_1(z_1, z_2)] = \mathbb{E}[\mathbb{E}(Y_1 \mid Z_1 = z_1, Z_2 = z_2, \mathbf{U})],$$

where the outer expectation is with respect to \mathbf{U} . Therefore, local and interference effects are identified while controlling for the local and neighborhood covariate.

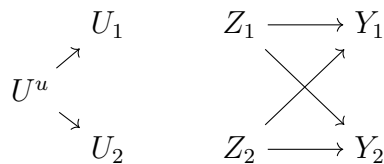
2. This is a scenario where interference is absent, and we can denote potential outcomes for Unit 1 based only on the treatment of the unit itself, $Y_1(z_1, z_2) = Y_1(z_1)$. The neighborhood exposure, Z_2 is a collider on the backdoor path $Z_1 \leftarrow Z^u \rightarrow Z_2 \leftarrow U_2 \rightarrow Y_1$. Therefore, When Z_2 is conditioned on, this backdoor path is open. This implies that $Z_1 \not\perp\!\!\!\perp Y_1(z_1) \mid Z_2, U_1$ and local effects are not identified.

□

B.3 Graph 3c: Spatial interference

The definitions of the local and interference effects $\lambda_i(\pi)$ and $\iota_i(\pi)$ that appear in this subsection are given in Supplement A.1.

Propositions S.3 and S.5 refer to the case of Figure 3c with \mathbf{Z} not spatial. This case corresponds to the graph:



Proposition S.3. For variables with causal relationships depicted in Figure 3c, if Z is not spatial, then $\lambda_1(\pi)$ for $\pi = P(Z_2 = 1)$ is identifiable based on the difference of averages of Unit 1 outcomes for pairs with $Z_1 = 1$ and pairs with $Z_1 = 0$, i.e.,

$$\lambda_1(\pi) = \mathbb{E}(Y_1 \mid Z_1 = 1) - \mathbb{E}(Y_1 \mid Z_1 = 0)$$

The case for $\lambda_2(\pi')$, for $\pi' = P(Z_1 = 1)$ is symmetric.

Proof of Proposition S.3. Note that

$$\begin{aligned} \lambda_1(\pi) &= \mathbb{E}[\pi Y_1(1, 1) - \pi Y_1(0, 1) + (1 - \pi)Y_1(1, 0) - (1 - \pi)Y_1(0, 0)] \\ &= \mathbb{E}[\pi Y_1(1, 1) + (1 - \pi)Y_1(1, 0)] - \mathbb{E}[\pi Y_1(0, 1) + (1 - \pi)Y_1(0, 0)], \end{aligned}$$

so it suffices to identify $\mathbb{E}[\pi Y_1(z, 1) + (1 - \pi)Y_1(z, 0)]$, for $z = 0, 1$. The proof is similar to that on Page 566 of [Ogburn and VanderWeele \[2014\]](#).

$$\begin{aligned} &\mathbb{E}[\pi Y_1(z, 1) + (1 - \pi)Y_1(z, 0)] \\ &= \pi \mathbb{E}[Y_1(z, 1)] + (1 - \pi) \mathbb{E}[Y_1(z, 0)] \\ &= \pi \mathbb{E}[Y_1(z, 1) \mid Z_1 = z, Z_2 = 1] + (1 - \pi) \mathbb{E}[Y_1(z, 0) \mid Z_1 = z, Z_2 = 0] && \text{(Ignorability)} \\ &= \pi \mathbb{E}[Y_1 \mid Z_1 = z, Z_2 = 1] + (1 - \pi) \mathbb{E}[Y_1 \mid Z_1 = z, Z_2 = 0] \\ & && \text{(Consistency of potential outcomes)} \\ &= P(Z_2 = 1) \mathbb{E}[Y_1 \mid Z_1 = z, Z_2 = 1] + P(Z_2 = 0) \mathbb{E}[Y_1 \mid Z_1 = z, Z_2 = 0] \\ &= P(Z_2 = 1 \mid Z_1 = z) \mathbb{E}[Y_1 \mid Z_1 = z, Z_2 = 1] + P(Z_2 = 0 \mid Z_1 = z) \mathbb{E}[Y_1 \mid Z_1 = z, Z_2 = 0] \\ & && \text{(Treatment values are independent)} \\ &= \mathbb{E}[Y_1 \mid Z_1 = z]. \end{aligned}$$

□

Proposition S.4. For the variables' with causal dependence depicted in Figure 3c, when the exposure Z is spatial, the difference of averages of Unit 1 outcomes for pairs with $Z_1 = 1$ and pairs with $Z_1 = 0$ does *not* identify an interpretable local effect for Unit 1. Interpretable local causal effects for Unit 1 can be identified by adjusting for the neighbor's exposure.

Proof of Proposition S.4. Following the steps of the proof of Proposition S.3 backwards, we have that the average outcome of Unit 1 among pairs with $Z_1 = z$ estimates the quantity

$$\mathbb{E}(Y_1 \mid Z_1 = z) = P(Z_2 = 1 \mid Z_1 = z) \mathbb{E}[Y_1(z, 1)] + P(Z_2 = 0 \mid Z_1 = z) \mathbb{E}[Y_1(z, 0)]$$

where we used consistency of potential outcomes, and that $\mathbf{Z} \perp\!\!\!\perp Y_1(z_1, z_2)$ under the causal dependence depicted in the graph 3c. This quantity is the average outcome when Unit 1's treatment is set to z and Unit 2's treatment is equal to 1 with probability $P(Z_2 = 1 \mid Z_1 = z)$ and 0 otherwise.

Then, the contrast of average Unit 1 outcomes among pairs with $Z_1 = 1$ and $Z_1 = 0$ estimates the peculiar contrast

$$\begin{aligned} \mathbb{E}(Y_1 \mid Z_1 = 1) - \mathbb{E}(Y_1 \mid Z_1 = 0) &= \\ &= \{P(Z_2 = 1 \mid Z_1 = 1)\mathbb{E}[Y_1(1, 1)] + P(Z_2 = 0 \mid Z_1 = 1)\mathbb{E}[Y_1(1, 0)]\} \\ &\quad - \{P(Z_2 = 1 \mid Z_1 = 0)\mathbb{E}[Y_1(0, 1)] + P(Z_2 = 0 \mid Z_1 = 0)\mathbb{E}[Y_1(0, 0)]\}, \end{aligned}$$

where not only Unit 1's treatment changes from 1 to 0, but also the probability of treatment for Unit 2 changes. Therefore, it is unclear whether this estimated quantity has a causal interpretation. At the least, it does not isolate the effect of a change in Z_1 and cannot be interpreted as a local causal effect.

Since the ignorability of the (vector) exposure holds unconditionally, $\mathbf{Z} \perp\!\!\!\perp Y_1(z_1, z_2)$, we have that Unit 1's local effects defined in Section 2 can be identified when Z_2 is adjusted.

□

Remark S.1. When \mathbf{Z} is not spatial, $P(Z_2 = 1 \mid Z_1 = z) = P(Z_2 = 1)$, and Proposition S.4 reverts back to Proposition S.3. The results in Propositions S.3 and S.4 combined establish explicitly how, in this very simple case without any confounding, an identification strategy for local effects can be invalidated by statistical dependence in the exposure variable.

Proposition S.5. For variables with causal relationships depicted in Figure 3c, if \mathbf{Z} is not spatial, then $\iota_1(\pi)$ for $\pi = P(Z_1 = 1)$ is identifiable based on the difference of averages of Unit 1 outcomes for pairs with $Z_2 = 1$ and pairs with $Z_2 = 0$. The case for $\iota_2(\pi')$, for $\pi' = P(Z_2 = 1)$ is symmetric.

The proof of Proposition S.5 is identical to the proof of Proposition S.3, hence it is omitted.

B.4 Graph 3d: Interference with spatial predictor of the exposure

Proposition S.6. For the variables with causal relationships depicted in Figure 3d, the difference of averages of Unit 1 outcomes for pairs with $Z_1 = 1$ and pairs with $Z_1 = 0$ conditionally on U_1 and unconditionally identify different quantities, none of which is an interpretable causal effect.

Proof of Proposition S.6. We consider again two estimators, one of which is unconditional and the other is conditional on U_1 . These estimators are of the form

$$\hat{\tau} = \mathbb{E}(Y_1 \mid Z_1 = 1) - \mathbb{E}(Y_1 \mid Z_1 = 0),$$

and

$$\hat{\tau}^{|U} = \mathbb{E}[\mathbb{E}(Y_1 | Z_1 = 1, U_1) - \mathbb{E}(Y_1 | Z_1 = 0, U_1)],$$

respectively, where for the second estimator the outer expectation is with respect to the distribution of U_1 across pairs.

For the unconditional estimator, $\hat{\tau}$, since $\mathbf{Z} \perp\!\!\!\perp Y_1(z_1, z_2)$ under the causal dependencies represented in 3d, we can again derive that

$$\begin{aligned} \hat{\tau} &= \mathbb{E}(Y_1 | Z_1 = 1) - \mathbb{E}(Y_1 | Z_1 = 0) \\ &= \{P(Z_2 = 1 | Z_1 = 1)\mathbb{E}[Y_1(1, 1)] + P(Z_2 = 0 | Z_1 = 1)\mathbb{E}[Y_1(1, 0)]\} \\ &\quad - \{P(Z_2 = 1 | Z_1 = 0)\mathbb{E}[Y_1(0, 1)] + P(Z_2 = 0 | Z_1 = 0)\mathbb{E}[Y_1(0, 0)]\}, \end{aligned}$$

identically to the derivations in the proof of Proposition S.4.

Furthermore, since $\mathbf{Z} \perp\!\!\!\perp Y_1(z_1, z_2) | U_1$ also holds, we can similarly derive that

$$\begin{aligned} \mathbb{E}[\mathbb{E}(Y_1 | Z_1 = z, U_1)] &= \\ &= \mathbb{E}\{P(Z_2 = 1 | Z_1 = z, U_1) \mathbb{E}[Y_1(z, 1) | U_1] + \\ &\quad + P(Z_2 = 0 | Z_1 = z, U_1) \mathbb{E}[Y_1(z, 0) | U_1]\} \\ &= \mathbb{E}[P(Z_2 = 1 | Z_1 = z, U_1)] \mathbb{E}[Y_1(z, 1)] + \\ &\quad + \mathbb{E}[P(Z_2 = 0 | Z_1 = z, U_1)] \mathbb{E}[Y_1(z, 0)], \end{aligned}$$

where, in the last equation, we have used the fact that U_1 does not predict Y_1 except through Z . Therefore the (conditional) contrast of average outcomes, $\hat{\tau}^{|U}$ estimates

$$\begin{aligned} \hat{\tau}^{|U} &= \mathbb{E}[\mathbb{E}(Y_1 | Z_1 = 1, U_1)] - \mathbb{E}[\mathbb{E}(Y_1 | Z_1 = 0, U_1)] \\ &= \{\mathbb{E}[P(Z_2 = 1 | Z_1 = 1, U_1)] \mathbb{E}[Y_1(1, 1)] + \mathbb{E}[P(Z_2 = 0 | Z_1 = 1, U_1)] \mathbb{E}[Y_1(1, 0)]\} - \\ &\quad - \{\mathbb{E}[P(Z_2 = 1 | Z_1 = 0, U_1)] \mathbb{E}[Y_1(0, 1)] + \mathbb{E}[P(Z_2 = 0 | Z_1 = 0, U_1)] \mathbb{E}[Y_1(0, 0)]\}. \end{aligned}$$

In general, it holds that

$$P(Z_2 = 1 | Z_1 = z) \neq \mathbb{E}[P(Z_2 = 1 | Z_1 = z, U_1)],$$

since the outer expectation on the right-hand side is with respect to the (marginal) distribution of U_1 , rather than the distribution of U_1 given $Z_1 = z$. Since these two quantities are different, in general it holds that $\hat{\tau} \neq \hat{\tau}^{|U}$. Therefore, the conditional and unconditional estimators estimate different quantities.

The proof that none of these estimate an interpretable causal effect is identical to the one in the proof of Proposition S.4, and it relates to the fact that these contrast consider a distribution for Z_2 that changes based on the value of Z_1 . \square

Remark S.2. From the proof of Proposition S.6, we can identify some interesting cases where the conditional and unconditional estimators estimate the same quantity, or they return interpretable local causal effects:

- When Z is not spatial, we have that

$$\mathbb{E}[P(Z_2 = 1 \mid Z_1 = z, U_1)] = \mathbb{E}[P(Z_2 = 1 \mid U_1)] = P(Z_2 = 1),$$

and therefore the conditional estimator, $\hat{\tau}^{|U}$, estimates the interpretable local causal effect $\lambda_1(P(Z_2 = 1))$.

- When Z is not spatial, but the spatial predictor U is present, $P(Z_2 = 1 \mid Z_1 = z) \neq P(Z_2 = 1)$, and the unconditional estimator, $\hat{\tau}$, still fails to estimate an interpretable causal effect.
- When U is not spatial, $\mathbb{E}[P(Z_2 = 1 \mid Z_1 = z, U_1)] = P(Z_2 = 1 \mid Z_1 = z)$, and the two estimators estimate the same quantity.

B.5 Graph 3e: Direct spatial confounding and interference

Proposition S.7. When the variables' causal relationships are depicted in Figure 3e,

1. Controlling for the local confounder and neighborhood exposure suffices to identify local effects.
2. Failing to adjust for the local confounder or the neighborhood exposure returns estimates that cannot be interpreted as causal effects.

Proof of Proposition S.7.

1. The local confounder blocks all backdoor paths from Z into Y_1 . As a result, all potential outcomes of the form $\mathbb{E}[Y_1(z_1, z_2)]$, and hence local (and interference) effects, can be identified.
2. Without conditioning on U_1 , there is a backdoor path from the vector Z to the outcome Y_1 , and we have that $Z \not\perp\!\!\!\perp Y_1(z_1, z_2)$. Therefore, local (or interference) effects cannot be identified.

Without conditioning on Z_2 , this setting is almost identical to the one discussed in Proposition S.6 where U_1 is conditioned on or not, and estimated quantities cannot be interpreted as causal effects.

\square

Next, we focus on identification of interpretable causal effects when the exposure is not spatial. Proposition S.8 shows that, when \mathbf{Z} is not spatial, one would need to adjust only for the local confounder in order to acquire interpretable local causal effects, even if interference is present. First, we define these *new* type of interpretable effects.

We define conditional average local effects. First, let

$$\lambda_i(z; u_i) = \mathbb{E}[Y_i(z_i = 1, z_j = z) - Y_i(z_i = 0, z_j = 0) \mid U_i = u_i]$$

denote the expected change in unit i 's outcome for changes in its own treatment when the neighbor's treatment is set to z , among clusters with $U_i = u_i$. This is the equivalent to the local effects defined in (1), where we now also condition on the unit's covariate values.

We also consider expected conditional average local effects, where we average over a distribution for the neighbor's treatment. Specifically, let $\pi(u_i) = P(Z_j = 1 \mid U_i = u_i)$. We define

$$\lambda_i(\pi(u_i); u_i) = \pi(u_i)\lambda_i(1; u_i) + (1 - \pi(u_i))\lambda_i(0; u_i),$$

representing the average change in unit i 's outcome among clusters with $U_i = u_i$ for changes in unit i 's own treatment, and when the treatment of its neighbor is distributed according to $\pi(\cdot)$. These effects are the conditional equivalent to effects $\lambda_i(\pi)$ in Supplement A.1.

Proposition S.8. When the variables' causal relationships can be described in the graph of Figure 3e, if \mathbf{Z} is not spatial, it holds that

$$\mathbb{E}_{U_1}[\lambda_1(\pi(U_1); U_1)] = \mathbb{E}_{U_1}[\mathbb{E}(Y_1 \mid Z_1 = 1, U_1) - \mathbb{E}(Y_1 \mid Z_1 = 0, U_1)]$$

The case for $\mathbb{E}_{U_2}[\lambda_2(\pi'(U_2); U_2)]$, for $\pi'(u_2) = P(Z_1 = 1 \mid U_2 = u_2)$ is symmetric.

Proof of Proposition S.8. We follow steps that are similar to those in the proof of Proposition S.3. However, here, we have to account for the fact that we average over a distribution of $\pi(U_1)$.

$$\begin{aligned} \mathbb{E}_{U_1} [\mathbb{E}(Y_1 \mid Z_1 = 1, U_1) - \mathbb{E}(Y_1 \mid Z_1 = 0, U_1)] &= \\ &= \mathbb{E}_{U_1} \left\{ \left[\mathbb{E}(Y_1 \mid Z_1 = 1, Z_2 = 1, U_1) P(Z_2 = 1 \mid Z_1 = 1, U_1) + \right. \right. \\ &\quad \left. \mathbb{E}(Y_1 \mid Z_1 = 1, Z_2 = 0, U_1) P(Z_2 = 0 \mid Z_1 = 1, U_1) \right] - \\ &\quad \left[\mathbb{E}(Y_1 \mid Z_1 = 0, Z_2 = 1, U_1) P(Z_2 = 1 \mid Z_1 = 0, U_1) + \right. \\ &\quad \left. \mathbb{E}(Y_1 \mid Z_1 = 0, Z_2 = 0, U_1) P(Z_2 = 0 \mid Z_1 = 0, U_1) \right] \left. \right\} \\ &= \mathbb{E}_{U_1} \left\{ \left[\mathbb{E}(Y_1(1, 1) \mid Z_1 = 1, Z_2 = 1, U_1) P(Z_2 = 1 \mid Z_1 = 1, U_1) + \right. \right. \\ &\quad \left. \mathbb{E}(Y_1(1, 0) \mid Z_1 = 1, Z_2 = 0, U_1) P(Z_2 = 0 \mid Z_1 = 1, U_1) \right] - \end{aligned}$$

$$\begin{aligned}
& [\mathbb{E}(Y_1(0, 1) \mid Z_1 = 0, Z_2 = 1, U_1) P(Z_2 = 1 \mid Z_1 = 0, U_1) + \\
& \quad \mathbb{E}(Y_1(0, 0) \mid Z_1 = 0, Z_2 = 0, U_1) P(Z_2 = 0 \mid Z_1 = 0, U_1)] \} \\
& \quad \text{(Consistency of potential outcomes)} \\
& = \mathbb{E}_{U_1} \{ [\mathbb{E}(Y_1(1, 1) \mid U_1) P(Z_2 = 1 \mid Z_1 = 1, U_1) + \mathbb{E}(Y_1(1, 0) \mid U_1) P(Z_2 = 0 \mid Z_1 = 1, U_1)] - \\
& \quad [\mathbb{E}(Y_1(0, 1) \mid U_1) P(Z_2 = 1 \mid Z_1 = 0, U_1) + \mathbb{E}(Y_1(0, 0) \mid U_1) P(Z_2 = 0 \mid Z_1 = 0, U_1)] \} \\
& \quad \text{(Ignorability } Z_1, Z_2 \perp\!\!\!\perp Y_1(z_1, z_2) \mid U_1 \text{ implied by the graph 3e)} \\
& = \mathbb{E}_{U_1} \{ [\mathbb{E}(Y_1(1, 1) \mid U_1) P(Z_2 = 1 \mid U_1) + \mathbb{E}(Y_1(1, 0) \mid U_1) P(Z_2 = 0 \mid U_1)] - \\
& \quad [\mathbb{E}(Y_1(0, 1) \mid U_1) P(Z_2 = 1 \mid U_1) + \mathbb{E}(Y_1(0, 0) \mid U_1) P(Z_2 = 0 \mid U_1)] \} \\
& \quad (Z_1 \perp\!\!\!\perp Z_2 \mid U_1 \text{ according to the graph 3e)} \\
& = \mathbb{E}_{U_1} \{ [\mathbb{E}(Y_1(1, 1) \mid U_1) \pi(U_1) + \mathbb{E}(Y_1(1, 0) \mid U_1) (1 - \pi(U_1))] - \\
& \quad [\mathbb{E}(Y_1(0, 1) \mid U_1) \pi(U_1) + \mathbb{E}(Y_1(0, 0) \mid U_1) (1 - \pi(U_1))] \} \\
& = \mathbb{E}_{U_1} [\lambda_1(\pi(U_1); U_1)]
\end{aligned}$$

□

We can define and identify interference effects similarly, without adjusting for the local exposure value.

Supplement C. Motivating simulation studies

C.1 Motivating simulation study with paired data

To illustrate the points made in Section 2.3 and show how interference and spatial confounding can manifest as each other and affect estimation of local and interference effects, we perform a small simulation study. We simulate pairs of \mathbf{U} from a bivariate Normal distribution with mean 0, and covariance matrix $\Sigma_U = \begin{pmatrix} 1 & \phi_U \\ \phi_U & 1 \end{pmatrix}$. We also simulate a bivariate normal error term $\epsilon_Z = (\epsilon_{Z,1}, \epsilon_{Z,2})$ with marginal variances equal to 1 and correlation parameter ϕ_Z . The binary exposure is generated from a Bernoulli distribution with a logistic link function and linear predictor $\beta_{UZ}U_i + \epsilon_{Z,i}$. Higher values of ϕ_U, ϕ_Z correspond to stronger inherent spatial dependence for \mathbf{U} and \mathbf{Z} . The outcome is generated independently across locations from a normal distribution with mean $\beta_Z Z_i + \beta_{\bar{Z}} \bar{Z}_i + \beta_U U_i + \beta_{\bar{U}} \bar{U}_i$ and variance 1, where \bar{Z}_i and \bar{U}_i represent the value of the exposure and the covariate for the neighbor of location i , respectively. Under this model, β_Z and $\beta_{\bar{Z}}$ correspond to the local and interference effects, respectively. We consider the six different scenarios presented in Figure 3 by setting different parameters to zero. We simulate 300 data sets of 200 pairs each, and fit

ordinary least squares (OLS) using different sets of predictor variables. The data generating model and hyperparameters for each of these scenarios are listed in Table S.1, along with the bias for the OLS estimators of β_Z and $\beta_{\bar{Z}}$.

In the presence of only direct spatial confounding (Scenario 3a), we see that failing to adjust for the local spatial confounder returns biased interference effect estimates ($\beta_{\bar{Z}}$ in the model with Z, \bar{Z} in Table S.1). Therefore, in the presence of inherently spatial data, adjusting for spatial confounders is crucial for learning interference effects, even if spatial confounding is direct only. When spatial confounding is both direct and indirect (Scenario 3b), adjusting only for the local spatial confounder and exposure values can still return misleading interference effects ($\beta_{\bar{Z}}$ in the model with Z, \bar{Z}, U), and it is necessary to also account for the neighbor’s covariate value. In the presence of interference (Scenario 3c) and when the exposure is inherently spatial, the local effect estimator is biased when the neighbor’s exposure value is not conditioned on, and the bias is larger for stronger spatial dependence. Instead, local and interference effects can be unbiasedly estimated when they are considered simultaneously ($\beta_Z, \beta_{\bar{Z}}$ in the model with Z, \bar{Z}). In Scenario 3d, the local effect of the exposure for unit i is biased regardless of whether U_i is adjusted for or not. At the same time, the estimates when U_i is included in the model or not are substantially different, which could be interpreted as U_i confounding the local effect. Therefore, in this scenario, the inherent spatial structure in the confounders and exposure could lead to interference being mistakenly interpreted as spatial confounding. In Scenario 3e, we see that when the exposure is not inherently spatial ($\phi_Z = 0$), we can learn local effects without adjusting for the neighbor’s exposure. However, this estimator is biased when the exposure has an inherent spatial structure, illustrating practically that spatial dependencies can hinder some analyses invalid if not properly taken into account. Of course, when all the possible dependencies are present in Scenario 3f, one would need to condition on local and neighborhood covariates to properly estimate local and interference effects. The estimator that account for all of local and neighborhood exposure and confounding values returns unbiased effect estimates across all scenarios.

C.2 Motivating simulation study in a setting with one spatial network of observations

We consider a graph with n nodes. We assume that this graph is a line graph, in that the first and last nodes are connected only to the second and second to last, respectively, and node i is connected to nodes $i - 1$ and $i + 1$ for $i = 2, 3, \dots, n - 1$. This implies the following adjacency and degree

Table S.1: Motivating Simulation Study with Paired Data. For the graphs of Figure 3, we illustrate the induced biases in estimating local and interference causal effects due to spatial dependencies. In these simulations, the parameters that drive the data generative mechanism are $\phi_U, \phi_Z, \beta_{UZ}, \beta_Z, \beta_{\bar{Z}}, \beta_U, \beta_{\bar{U}}$. The different scenarios of Figure 3 correspond to different set of parameters fixed at 0, shown below. Unless otherwise noted, the parameters are fixed at $\phi_U = 0.7, \phi_Z = 0.5, \beta_{UZ} = 1, \beta_Z = 1, \beta_{\bar{Z}} = 0.8, \beta_U = 1, \beta_{\bar{U}} = 0.5$. We generate 300 data sets of 200 pairs each. We regress the outcome on a different set of variables (columns), and report the bias of the OLS estimator for the local effect estimator, β_Z , and the interference effect estimator, $\beta_{\bar{Z}}$, when \bar{Z} is included in the conditioning set. Values are rounded to the third decimal point, and those in **bold** are discussed in the main text.

True Model	Alternative spatial parameters	Conditioning set & estimated parameter							
		(Z)	(Z, U)	(Z, \bar{Z})		(Z, \bar{Z}, U)		(Z, \bar{Z}, U, \bar{U})	
		β_Z	β_Z	β_Z	$\beta_{\bar{Z}}$	β_Z	$\beta_{\bar{Z}}$	β_Z	$\beta_{\bar{Z}}$
3a		$\beta_{\bar{Z}} = 0$ and $\beta_{\bar{U}} = 0$							
		0.726	-0.003	0.660	0.406	-0.003	-0.002	-0.002	0.000
3b		$\beta_{\bar{Z}} = 0$							
		0.983	0.002	0.863	0.737	-0.013	0.198	-0.002	0.000
3c		$\beta_{UZ} = 0$ and $\beta_U = \beta_{\bar{U}} = 0$							
	$\phi_z = 0.7$	0.152	0.087	0.001	-0.002	-0.001	-0.003	0.000	-0.002
	$\phi_z = 0.5$	0.129	0.060	-0.001	-0.001	-0.003	-0.002	-0.002	0.000
	$\phi_z = 0.3$	0.105	0.032	-0.002	0.001	-0.003	0.000	-0.003	0.001
3d		$\beta_U = 0$ and $\beta_{\bar{U}} = 0$							
	$\beta_{UZ} = 1.5$	0.173	0.052	0.000	0.001	-0.002	0.000	-0.002	0.003
	$\beta_{UZ} = 1$	0.129	0.060	-0.001	-0.001	-0.003	-0.002	-0.002	0.000
	$\beta_{UZ} = 0.5$	0.083	0.061	-0.004	-0.003	-0.006	-0.004	-0.005	-0.003
3e		$\beta_{\bar{U}} = 0$							
	$\phi_z = 0.5$	0.856	0.060	0.660	0.406	-0.003	-0.002	-0.002	0.000
	$\phi_z = 0$	0.800	-0.001	0.684	0.445	0.000	-0.003	0.000	-0.001
3f		1.113	0.064	0.863	0.737	-0.013	0.198	-0.002	0.000

matrices:

$$A = \begin{pmatrix} 0 & 1 & 0 & 0 & \dots & 0 & 0 & 0 \\ 1 & 0 & 1 & 0 & \dots & 0 & 0 & 0 \\ 0 & 1 & 0 & 1 & \dots & 0 & 0 & 0 \\ & \vdots & & & & \vdots & & \\ 0 & 0 & 0 & 0 & \dots & 1 & 0 & 1 \\ 0 & 0 & 0 & 0 & \dots & 0 & 1 & 0 \end{pmatrix} \quad \text{and} \quad D = \begin{pmatrix} 1 & 0 & 0 & \dots & 0 & 0 \\ 0 & 2 & 0 & \dots & 0 & 0 \\ 0 & 0 & 2 & \dots & 0 & 0 \\ & \vdots & & \ddots & \vdots & \\ 0 & 0 & 0 & \dots & 2 & 0 \\ 0 & 0 & 0 & \dots & 0 & 1 \end{pmatrix}.$$

We generate $\mathbf{U} = (U_1, U_2, \dots, U_n)$ and $\mathbf{Z} = (Z_1, Z_2, \dots, Z_n)$ simultaneously from a multivariate normal distribution as follows

$$\begin{pmatrix} \mathbf{U} \\ \mathbf{Z} \end{pmatrix} \sim N_{2n} \left(\mathbf{0}_{2n}, \begin{pmatrix} G & Q \\ Q & H \end{pmatrix}^{-1} \right),$$

where $\mathbf{0}_{2n}$ is a vector of length $2n$ of all 0s. We specify G and H according to a conditional autoregressive distribution as $G = \tau_U^2(D - \phi_U A)$ and $H = \tau_Z^2(D - \phi_Z A)$. Then, Q is specified to be diagonal with elements $Q_{ii} = -\rho\sqrt{G_{ii}H_{ii}}$. Note that different values of ϕ for the same value of τ lead to different marginal variances for the entries of \mathbf{U} and \mathbf{Z} .

We exclude measured covariates for simplicity. Once \mathbf{U} and \mathbf{Z} are generated, the outcome is generated according to the model (5), where $\epsilon \sim N(0, 1)$ independent. Unless otherwise specified, the hyperparameters for these simulations are set to the values reported in Table S.2.

Supplement D. Identifiability of model parameters

Proof of Theorem 1. Consider a spatial network of observations that are organized on a ring graph, with symmetric adjacency matrix $A_{ij} = 1$ if $|i - j| = 1$, ($i = 1, j = n$) and ($i = n, j = 1$), and 0 otherwise. Intuitively, under this structure, each unit has two neighbors, the ones with adjacent indices, and units 1 and n are connected.

Without loss of generality, we consider the case without measured covariates and where the exposure has mean 0. We show that all coefficients, parameters in the precision matrix, and residual variance are identifiable, hence the causal effects of interest are also identifiable.

A few useful derivations

- We can write $\bar{\mathbf{U}} = D^{-1}A\mathbf{U}$ and $\bar{\mathbf{Z}} = D^{-1}A\mathbf{Z}$, where D is the degree and A is the adjacency matrix.

Table S.2: Motivating Simulation Study with One Interconnected Network. Unless otherwise noted, the parameters are fixed at $\phi_U = 0.6$, $\phi_Z = 0.4$, $\tau_U = \tau_Z = 1$, $\rho = 0.35$, $\beta_Z = 1$, $\beta_{\bar{Z}} = 0.8$, $\beta_U = 1$, $\beta_{\bar{U}} = 0.5$. We generate 200 data sets with $n = 100$. We regress the outcome on a different set of variables (columns), and report the bias of the OLS estimator for the local effect estimator, β_Z , and the interference effect estimator, $\beta_{\bar{Z}}$, when \bar{Z} is included in the conditioning set. Values are rounded to the third decimal point. We bold the entries corresponding to the same cells as in Table S.1. The qualitative conclusions remain unchanged.

True Model	Alternative spatial parameters	Conditioning set & estimated parameter							
		(Z)	(Z, U)	(Z, \bar{Z})		(Z, \bar{Z}, U)		(Z, \bar{Z}, U, \bar{U})	
		β_Z	β_Z	β_Z	$\beta_{\bar{Z}}$	β_Z	$\beta_{\bar{Z}}$	β_Z	$\beta_{\bar{Z}}$
3a		$\beta_Z = 0$ and $\beta_{\bar{U}} = 0$							
		0.550	-0.005	0.428	0.370	-0.007	0.006	-0.007	-0.004
3b		$\beta_{\bar{Z}} = 0$							
		0.683	0.045	0.489	0.595	-0.008	0.237	-0.013	0.030
3c		$\rho = 0$ and $\beta_U = \beta_{\bar{U}} = 0$							
	$\phi_z = 0.6$	0.437	0.334	-0.012	0.000	-0.007	0.002	-0.007	0.011
	$\phi_z = 0.4$	0.261	0.193	-0.002	-0.008	0.003	-0.004	0.002	-0.007
	$\phi_z = 0.2$	0.151	0.088	0.006	-0.002	0.002	-0.005	0.003	0.000
3d		$\beta_U = 0$ and $\beta_{\bar{U}} = 0$							
	$\rho = 0.15$	0.183	0.170	0.003	0.003	0.004	0.005	0.004	0.002
	$\rho = 0.35$	0.275	0.186	0.011	-0.012	0.004	-0.018	0.004	-0.018
	$\rho = 0.45$	0.431	0.246	0.014	-0.009	0.013	-0.011	0.012	-0.011
3e		$\beta_{\bar{U}} = 0$							
	$\phi_Z = 0.4$	0.838	0.195	0.456	0.345	0.001	0.021	0.001	0.019
	$\phi_Z = 0$	0.501	-0.010	0.444	0.283	0.001	-0.017	0.001	-0.019
3f		0.973	0.222	0.507	0.611	-0.008	0.209	-0.014	-0.002

- We have that

$$\begin{pmatrix} G & Q \\ Q^\top & H \end{pmatrix}^{-1} = \begin{pmatrix} G^{-1} + G^{-1}Q(H - Q^\top G^{-1}Q)^{-1}Q^\top G^{-1} & -G^{-1}Q(H - Q^\top G^{-1}Q)^{-1} \\ -(H - Q^\top G^{-1}Q)^{-1}Q^\top G^{-1} & (H - Q^\top G^{-1}Q)^{-1} \end{pmatrix},$$

and using the known formulas for the multivariate normal distribution, we have that

$$\mathbf{U} \mid \mathbf{Z} \sim N(-G^{-1}Q\mathbf{Z}, G^{-1}).$$

- The diagonal elements of the diagonal matrix Q are $Q_{ii} = -\rho\sqrt{g_{ii}h_{ii}}$. Under the CAR form of $G = \tau_U^2(D - \phi_U A)$ and $H = \tau_Z^2(D - \phi_Z A)$, we have that $Q_{ii} = -2\rho\tau_U\tau_Z$. These imply that

$$G^{-1}Q = -2\rho\tau_U\tau_Z G^{-1}.$$

- Putting these together, we have that

$$\begin{aligned} \mathbb{E}(\mathbf{Y} \mid \mathbf{Z}) &= \beta_Z \mathbf{Z} + \beta_{\bar{Z}} \bar{\mathbf{Z}} + \mathbb{E}[\mathbf{U} \mid \mathbf{Z}] + \beta_{\bar{U}} \mathbb{E}[\bar{\mathbf{U}} \mid \mathbf{Z}] \\ &= \beta_Z \mathbf{Z} + \beta_{\bar{Z}} D^{-1} A \mathbf{Z} - G^{-1} Q \mathbf{Z} + \beta_{\bar{U}} D^{-1} A (-G^{-1} Q \mathbf{Z}) \\ &= \beta_Z \mathbf{Z} + \beta_{\bar{Z}} (D^{-1} A \mathbf{Z}) + 2\rho\tau_U\tau_Z (G^{-1} \mathbf{Z}) + 2\rho\tau_U\tau_Z \beta_{\bar{U}} (D^{-1} A G^{-1} \mathbf{Z}). \end{aligned} \quad (\text{S.1})$$

and that

$$\begin{aligned} \text{Var}(\mathbf{Y} \mid \mathbf{Z}) &= \text{Var}[(I_n + \beta_{\bar{U}} D^{-1} A) \mathbf{U} \mid \mathbf{Z}] + \sigma_Y^2 I_n \\ &= (I_n + \beta_{\bar{U}} D^{-1} A) \text{Var}(\mathbf{U} \mid \mathbf{Z}) (I_n + \beta_{\bar{U}} D^{-1} A)^\top + \sigma_Y^2 I_n \\ &= (I_n + \beta_{\bar{U}} D^{-1} A) G^{-1} (I_n + \beta_{\bar{U}} D^{-1} A)^\top + \sigma_Y^2 I_n, \end{aligned} \quad (\text{S.2})$$

where

$$I_n + \beta_{\bar{U}} D^{-1} A = \begin{pmatrix} 1 & \frac{\beta_{\bar{U}}}{2} & & \cdots & & \frac{\beta_{\bar{U}}}{2} \\ \frac{\beta_{\bar{U}}}{2} & 1 & \frac{\beta_{\bar{U}}}{2} & & \cdots & \\ & \frac{\beta_{\bar{U}}}{2} & 1 & \frac{\beta_{\bar{U}}}{2} & \cdots & \\ & & & \vdots & & \\ & & & \cdots & \frac{\beta_{\bar{U}}}{2} & 1 & \frac{\beta_{\bar{U}}}{2} \\ \frac{\beta_{\bar{U}}}{2} & & & \cdots & \frac{\beta_{\bar{U}}}{2} & 1 \end{pmatrix}$$

Theorem 1 of [Schnell and Papadogeorgou \[2020\]](#) shows that we can identify whether $\rho\phi_U = 0$ or not based on \mathbf{Z} . If $\rho\phi_U \neq 0$, they show that $(\tau_Z, \phi_Z, \phi_U, |\rho|)$ are identifiable. Their theorem applies here directly since their results are based on the same specification of the joint distribution (\mathbf{Z}, \mathbf{U}) on the ring graph.

Our proof deviates from theirs on the specification of the outcome structure and, as a result, the identifiability results for the remaining parameters. These differences stem from allowing for potential interference effects and for including additional parameters on the unmeasured spatial confounder due to non-local confounding, which leads to the inclusion of additional terms and additional unknown parameters in the distribution of \mathbf{Y} given \mathbf{Z} in equations (S.1) and (S.2).

In linear models, expectations and variances are separately identifiable. So we can identify $\text{Var}(\mathbf{Y} \mid \mathbf{Z})$ and $\mathbb{E}(\mathbf{Y} \mid \mathbf{Z})$.

Identifiability of parameters from $\text{Var}(\mathbf{Y} \mid \mathbf{Z})$ We acquire the form of the entries in G^{-1} as $n \rightarrow \infty$ based on Theorem 4 in the Supplementary Materials of Schnell and Papadogeorgou [2020]. Let entry (i, j) of matrix G^{-1} be denoted by g_{ij} . Then, we have that

$$\lim_{n \rightarrow \infty} g_{ij} = \frac{\tau_U^2}{2\sqrt{1 - \phi_U^2}} \left(\frac{\phi_U}{1 + \sqrt{1 - \phi_U^2}} \right)^{|i-j|} \quad (\text{S.3})$$

After some mundane matrix multiplications, we have that the entries of the variance in (S.2) can be written as

$$\begin{aligned} [\text{Var}(\mathbf{Y} \mid \mathbf{Z})]_{ij} &= g_{ij} + \frac{\beta_{\bar{U}}}{2} (g_{(i-1)j} + g_{(i+1)j} + g_{i(j-1)} + g_{i(j+1)}) + \\ &+ \frac{\beta_{\bar{U}}^2}{4} (g_{(i-1)(j-1)} + g_{(i-1)(j+1)} + g_{(i+1)(j-1)} + g_{(i+1)(j+1)}) + \sigma_Y^2 I(i = j). \end{aligned}$$

Therefore, we can write the limit of the (i, j) entry for the outcome conditional variance $\lim_{n \rightarrow \infty} \text{Var}(\mathbf{Y} \mid \mathbf{Z})_{ij}$ as a function of $k = |i - j|$:

- For $k = 0$, and $i = j$:

$$\begin{aligned} \lim_{n \rightarrow \infty} \text{Var}(\mathbf{Y} \mid \mathbf{Z})_{ij} &= \frac{\tau_U^2}{2\sqrt{1 - \phi_U^2}} + 4 \frac{\beta_{\bar{U}}}{2} \frac{\tau_U^2}{2\sqrt{1 - \phi_U^2}} \frac{\phi_U}{1 + \sqrt{1 - \phi_U^2}} \\ &+ 4 \frac{\beta_{\bar{U}}^2}{4} \frac{\tau_U^2}{2\sqrt{1 - \phi_U^2}} \left(\frac{\phi_U}{1 + \sqrt{1 - \phi_U^2}} \right)^2 + \sigma_Y^2 \\ &= \frac{\tau_U^2}{2\sqrt{1 - \phi_U^2}} \left[1 + 2\beta_{\bar{U}} \frac{\phi_U}{1 + \sqrt{1 - \phi_U^2}} + \beta_{\bar{U}}^2 \left(\frac{\phi_U}{1 + \sqrt{1 - \phi_U^2}} \right)^2 \right] + \sigma_Y^2 \\ &= \frac{\tau_U^2}{2\sqrt{1 - \phi_U^2}} \left[1 + \beta_{\bar{U}} \frac{\phi_U}{1 + \sqrt{1 - \phi_U^2}} \right]^2 + \sigma_Y^2 \end{aligned}$$

- For $k = 1$:

$$\begin{aligned}
\lim_{n \rightarrow \infty} \text{Var}(\mathbf{Y} \mid \mathbf{Z})_{ij} &= \frac{\tau_U^2}{2\sqrt{1-\phi_U^2}} \frac{\phi_U}{1+\sqrt{1-\phi_U^2}} + \\
&+ \frac{\beta_{\bar{U}}}{2} \left[2 \frac{\tau_U^2}{2\sqrt{1-\phi_U^2}} + 2 \frac{\tau_U^2}{2\sqrt{1-\phi_U^2}} \left(\frac{\phi_U}{1+\sqrt{1-\phi_U^2}} \right)^2 \right] + \\
&+ \frac{\beta_{\bar{U}}^2}{4} \left[3 \frac{\tau_U^2}{2\sqrt{1-\phi_U^2}} \frac{\phi_U}{1+\sqrt{1-\phi_U^2}} + \frac{\tau_U^2}{2\sqrt{1-\phi_U^2}} \left(\frac{\phi_U}{1+\sqrt{1-\phi_U^2}} \right)^3 \right] \\
&= \frac{\tau_U^2}{2\sqrt{1-\phi_U^2}} \left\{ \frac{\phi_U}{1+\sqrt{1-\phi_U^2}} + \beta_{\bar{U}} \left[1 + \left(\frac{\phi_U}{1+\sqrt{1-\phi_U^2}} \right)^2 \right] + \right. \\
&\quad \left. + \frac{\beta_{\bar{U}}^2}{4} \left[3 \frac{\phi_U}{1+\sqrt{1-\phi_U^2}} + \left(\frac{\phi_U}{1+\sqrt{1-\phi_U^2}} \right)^3 \right] \right\}
\end{aligned}$$

- For $k \geq 2$:

$$\begin{aligned}
\lim_{n \rightarrow \infty} \text{Var}(\mathbf{Y} \mid \mathbf{Z})_{ij} &= \\
&= \frac{\tau_U^2}{2\sqrt{1-\phi_U^2}} \left(\frac{\phi_U}{1+\sqrt{1-\phi_U^2}} \right)^k + \\
&+ \frac{\beta_{\bar{U}}}{2} \left[2 \frac{\tau_U^2}{2\sqrt{1-\phi_U^2}} \left(\frac{\phi_U}{1+\sqrt{1-\phi_U^2}} \right)^{k-1} + 2 \frac{\tau_U^2}{2\sqrt{1-\phi_U^2}} \left(\frac{\phi_U}{1+\sqrt{1-\phi_U^2}} \right)^{k+1} \right] + \\
&+ \frac{\beta_{\bar{U}}^2}{4} \left[2 \frac{\tau_U^2}{2\sqrt{1-\phi_U^2}} \left(\frac{\phi_U}{1+\sqrt{1-\phi_U^2}} \right)^k + \frac{\tau_U^2}{2\sqrt{1-\phi_U^2}} \left(\frac{\phi_U}{1+\sqrt{1-\phi_U^2}} \right)^{k-2} + \right. \\
&\quad \left. + \frac{\tau_U^2}{2\sqrt{1-\phi_U^2}} \left(\frac{\phi_U}{1+\sqrt{1-\phi_U^2}} \right)^{k+2} \right] \\
&= \frac{\tau_U^2}{2\sqrt{1-\phi_U^2}} \left\{ \left(\frac{\phi_U}{1+\sqrt{1-\phi_U^2}} \right)^k + \right. \\
&\quad + \beta_{\bar{U}} \left[\left(\frac{\phi_U}{1+\sqrt{1-\phi_U^2}} \right)^{k-1} + \left(\frac{\phi_U}{1+\sqrt{1-\phi_U^2}} \right)^{k+1} \right] + \\
&\quad \left. + \frac{\beta_{\bar{U}}^2}{4} \left[2 \left(\frac{\phi_U}{1+\sqrt{1-\phi_U^2}} \right)^k + \left(\frac{\phi_U}{1+\sqrt{1-\phi_U^2}} \right)^{k-2} + \left(\frac{\phi_U}{1+\sqrt{1-\phi_U^2}} \right)^{k+2} \right] \right\}
\end{aligned}$$

$$\begin{aligned}
&= \frac{\tau_U^2}{2\sqrt{1-\phi_U^2}} \left\{ \left(\frac{\phi_U}{1+\sqrt{1-\phi_U^2}} \right)^k + \right. \\
&\quad \left. + \beta_{\bar{U}} \left(\frac{\phi_U}{1+\sqrt{1-\phi_U^2}} \right)^{k-1} \left[1 + \left(\frac{\phi_U}{1+\sqrt{1-\phi_U^2}} \right)^2 \right] + \right. \\
&\quad \left. + \frac{\beta_{\bar{U}}^2}{4} \left(\frac{\phi_U}{1+\sqrt{1-\phi_U^2}} \right)^{k-2} \left[1 + \left(\frac{\phi_U}{1+\sqrt{1-\phi_U^2}} \right)^2 \right]^2 \right\} \\
&= \frac{\tau_U^2}{2\sqrt{1-\phi_U^2}} \left(\frac{\phi_U}{1+\sqrt{1-\phi_U^2}} \right)^{k-2} \left\{ \left(\frac{\phi_U}{1+\sqrt{1-\phi_U^2}} \right)^2 + \right. \\
&\quad \left. + \beta_{\bar{U}} \frac{\phi_U}{1+\sqrt{1-\phi_U^2}} \left[1 + \left(\frac{\phi_U}{1+\sqrt{1-\phi_U^2}} \right)^2 \right] + \right. \\
&\quad \left. + \frac{\beta_{\bar{U}}^2}{4} \left[1 + \left(\frac{\phi_U}{1+\sqrt{1-\phi_U^2}} \right)^2 \right]^2 \right\} \\
&= \frac{\tau_U^2}{2\sqrt{1-\phi_U^2}} \left(\frac{\phi_U}{1+\sqrt{1-\phi_U^2}} \right)^{k-2} \left\{ \frac{\phi_U}{1+\sqrt{1-\phi_U^2}} + \frac{\beta_{\bar{U}}}{2} \left[1 + \left(\frac{\phi_U}{1+\sqrt{1-\phi_U^2}} \right)^2 \right] \right\}^2
\end{aligned}$$

The parameter ϕ_U has been identified based on \mathbf{Z} . Identifiability of ϕ_U can also be achieved by comparing the variances of pairs at distance k and k' (when $k, k' \geq 2$), since for a pair (i, j) with distance k (e.g., $|i - j| = k$), and a pair (i', j') with distance k' (e.g., $|i' - j'| = k'$), we have that

$$\lim_{n \rightarrow \infty} \frac{\text{Var}(\mathbf{Y} | \mathbf{Z})_{i'j'}}{\text{Var}(\mathbf{Y} | \mathbf{Z})_{ij}} = \left(\frac{\phi_U}{1+\sqrt{1-\phi_U^2}} \right)^{k'-k}.$$

Therefore, the spatial parameter ϕ_U can be identified by studying how spatial correlation in the outcome attenuates with distance.

Once ϕ_U is identified, we can identify $\beta_{\bar{U}}$ by comparing the variances of pairs at distance 1 (pair (i, j) with $|i - j| = 1$) with that of pairs at distance 2 (pair (i', j') with $|i' - j'| = 2$), for which

$$\lim_{n \rightarrow \infty} \frac{\text{Var}(\mathbf{Y} | \mathbf{Z})_{i'j'}}{\text{Var}(\mathbf{Y} | \mathbf{Z})_{ij}} = \frac{\left\{ \frac{\phi_U}{1+\sqrt{1-\phi_U^2}} + \frac{\beta_{\bar{U}}}{2} \left[1 + \left(\frac{\phi_U}{1+\sqrt{1-\phi_U^2}} \right)^2 \right] \right\}^2}{\frac{\phi_U}{1+\sqrt{1-\phi_U^2}} + \beta_{\bar{U}} \left[1 + \left(\frac{\phi_U}{1+\sqrt{1-\phi_U^2}} \right)^2 \right] + \frac{\beta_{\bar{U}}^2}{4} \left[3 \frac{\phi_U}{1+\sqrt{1-\phi_U^2}} + \left(\frac{\phi_U}{1+\sqrt{1-\phi_U^2}} \right)^3 \right]}$$

is a bijective function of the parameter $\beta_{\bar{U}}$. Once $\beta_{\bar{U}}$ is identified, τ_U can be trivially identified based on the variance of pairs at distance 1 ($|i - j| = 1$). Subsequently, the residual variance σ_Y^2 can be identified based on the diagonal elements of the covariance matrix ($i = j$).

Identifiability of parameters from $\mathbb{E}(Y \mid Z)$ As long as the linear predictors in $\mathbb{E}(Y \mid Z)$ are not perfectly collinear, their corresponding coefficients are identifiable. These linear predictors are $Z, \bar{Z} = D^{-1}AZ, G^{-1}Z$, and $D^{-1}A(G^{-1}Z)$, where all parameters in G have been identified. We assume that the vector Z is not constant, and there is some variation in the exposure across units. Then, the local and neighborhood exposures are not perfectly correlated, and the first two predictors are not collinear. Note that a unit's entry in \bar{Z} is the average of the values in Z for its two neighbors. Based on the form of G^{-1} , we see that a unit's entry in $G^{-1}Z$ corresponds to a weighted average of entries in Z of all other units, with weights specified according to (S.3), which means that $G^{-1}Z$ is not collinear with the previous ones. Lastly, the same argument holds for $D^{-1}AG^{-1}Z$, as long as $G^{-1}Z$ is not constant across units.

From (S.1), we have that the coefficients $(\beta_Z, \beta_{\bar{Z}}, \rho\tau_U\tau_Z, \rho\tau_U\tau_Z\beta_{\bar{U}})$ are identifiable. Since τ_U and τ_Z have already been identified, we now have that the parameter ρ is identifiable as well.

□

Supplement E. Illustration of prior distributions

As discussed in Section 4.4, the prior specifications on the spatial parameters τ_U, τ_Z have implications on the implied prior on the the confounding strength due to U and the variance of the exposure Z , respectively. Here, we provide a simulation-based illustration for the implied prior properties discussed in the manuscript.

Before we delve into this illustration, we discuss briefly the matrices G, H in the joint precision matrix of Assumption 4, which in the absence of measured covariates states that

$$\begin{pmatrix} \mathbf{U} \\ \mathbf{Z} \end{pmatrix} \Big| \sim N_{2n} \left(\mathbf{0}_{2n}, \begin{pmatrix} G & Q \\ Q & H \end{pmatrix}^{-1} \right). \quad (\text{S.4})$$

Since the joint distribution is parameterized through its precision matrix, G^{-1} and H^{-1} are the marginal covariance matrices of \mathbf{U} and \mathbf{Z} , respectively, *only* when $\rho = 0$, and the distribution of \mathbf{U} when drawn from $N_n(\mathbf{0}_n, G^{-1})$ is different from the distribution of \mathbf{U} when drawn from (S.4) for $\rho \neq 0$. In our illustrations below, we will consider vectors \mathbf{U} and \mathbf{Z} which are drawn from $N_n(\mathbf{0}_n, G^{-1})$ and $N_n(\mathbf{0}_n, H^{-1})$, respectively, or simultaneously from (S.4) for $\rho \neq 0$.

E.1 Prior distribution for τ_U

The strength of a measured covariate C with variance 1 in the outcome model corresponds to the magnitude of its coefficient β_C , or (equivalently) the standard deviation of $\beta_C C_i$ across units i . Sim-

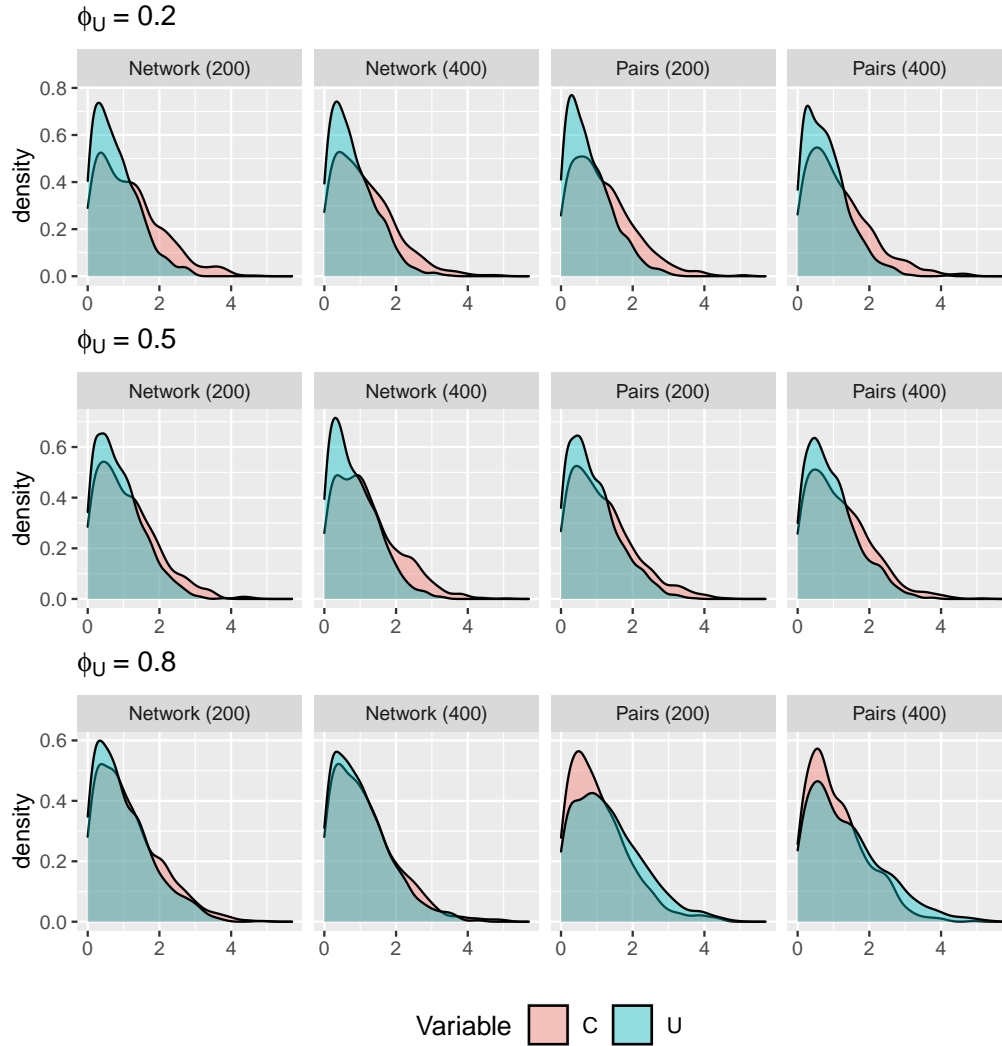


Figure S.1: Density plot for the implied prior distribution on the amount of outcome variability explained by a measured covariate and the unmeasured covariate U based on the prior distribution for τ_U . We consider network and pair data of sample sizes 200 and 400. U is generated from $N_n(\mathbf{0}_n, G^{-1})$ for τ_U sampled from its prior distribution and $\phi_U \in \{0.2, 0.5, 0.8\}$.

ilarly, since the coefficient of U_i is set to $\beta_U = 1$, the strength of the unmeasured U_i in the outcome model can be measured by the standard deviation of the unmeasured confounder. For network and paired data of sizes $n \in \{200, 400\}$, we performed the following procedure 1,000 times: (a) we drew $\beta_C \sim N(0, \sigma_{prior}^2)$, (b) we drew $1/\tau_U$ from the prior distribution described in Section 4.4, (c) we generated $\mathbf{U} = (U_1, U_2, \dots, U_n)$ from $N_n(\mathbf{0}_n, G^{-1})$ where G has a CAR structure with τ_U the one drawn at the previous step and $\phi_U \in \{0.2, 0.5, 0.8\}$. Each time, we calculated the absolute value of β_C and the standard deviation of U_i across i . Their distributions are shown in Figure S.1, using red for the measured covariate C and blue for the unmeasured covariate U . Considering that the outcome is standardized to have variance 1, the prior distribution for the strength of the unmeasured confounder in the outcome model allows for all reasonable values and it is relatively similar to the corresponding prior distribution for a measured covariate, across all configurations.

The two distributions are similar across all choices of σ_{prior}^2 we explored. Since prior distributions on model coefficients are well-explored and understood in the literature, the prior distribution for τ_U we designed can be used straightforwardly without requiring additional tuning. Specifically, a researcher can simply specify σ_{prior}^2 for the prior distribution of a coefficient in the outcome model, and our specification for the prior distribution of τ_U would automatically translate the choice of σ_{prior}^2 to an equivalent prior for the confounding strength of the unmeasured covariate.

E.2 Prior distribution for τ_Z

We also investigated the prior on the exposure’s variance as implied by the prior on τ_Z discussed in Section 4.4. We set the hypothesized marginal variance of \mathbf{Z} to $\tilde{s}_Z^2 = 1$ and the hypothesized residual variance of \mathbf{Z} to $\tilde{\sigma}_Z^2 = 0.5^2$. We repeated the following procedure 2,000 times: (a) we drew τ_Z from its prior distribution, (b) we generated \mathbf{Z} from $N_n(\mathbf{0}_n, H^{-1})$, where H is specified as CAR with τ_Z the draw from the previous step and $\phi_Z \in \{0.2, 0.5, 0.8\}$, and (c) we calculated the exposure variance across locations. We did so for network and paired data of sample sizes 200 and 400. The distribution of this variance is shown in Figure S.2, where the dashed vertical line represents the hypothesized residual variance of the exposure conditional on measured covariates, $\tilde{\sigma}_Z^2$. We see that the implied exposure variability takes values in the neighborhood of $\tilde{\sigma}_Z^2$, as expected.

E.3 Implied prior distributions when $\rho \neq 0$

Our prior distributions as described in Section 4.4 are designed based on approximations of the variability in the unmeasured covariate \mathbf{U} and the exposure \mathbf{Z} when the two variables are independent. Here, we illustrate using simulation that these prior distributions also imply reasonable prior distri-

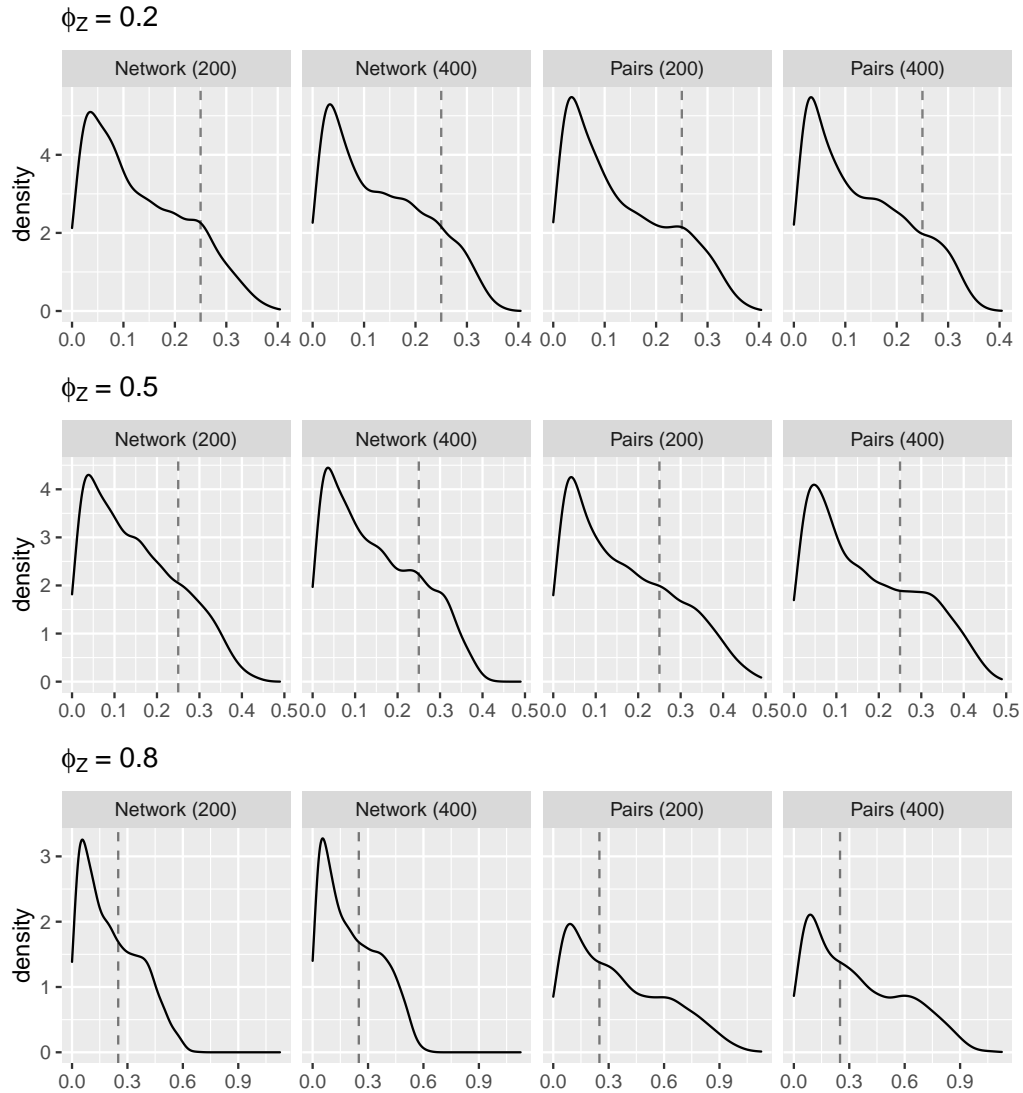


Figure S.2: Implied prior distribution on the exposure variability implied by the specified prior distribution for τ_Z . We consider network and pair data of sample sizes 200 and 400, and \mathbf{Z} is drawn from $N_n(\mathbf{0}_n, H^{-1})$ where H has a CAR structure with τ_Z sampled from its prior distribution and $\phi_Z \in \{0.2, 0.5, 0.8\}$.

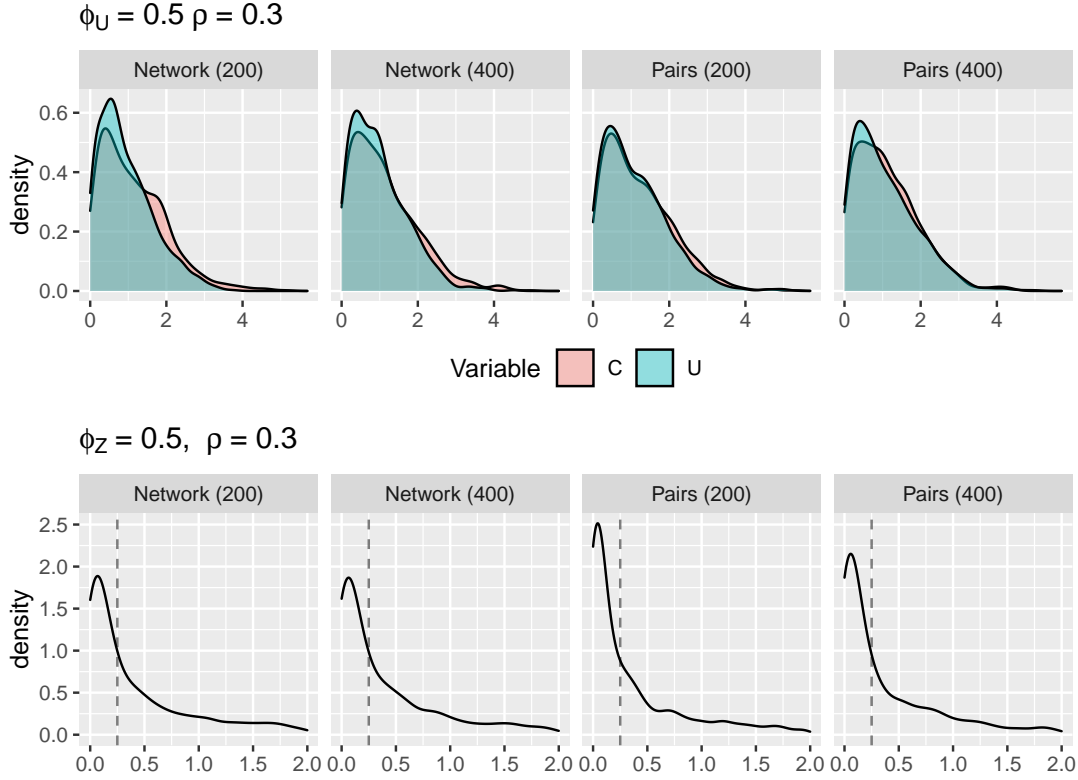


Figure S.3: Implied priors when the exposure and the unmeasured covariate are correlated according to Assumption 4 with $\phi_U = \phi_Z = 0.5$ and $\rho = 0.3$. Top: Prior distribution of predictive strength of a measured and the unmeasured covariates (equivalent of Figure S.1). Bottom: Prior distribution on the exposure variability (equivalent of Figure S.2).

butions on the strength of confounding due to U and the inherent exposure variability even when $\rho \neq 0$.

We performed the following procedure 1,000 times: (a) we drew τ_U and τ_Z from their prior distributions, (b) for these values and for $\phi_U = \phi_Z = 0.5$ and $\rho = 0.3$, we constructed the matrices G , H , and Q and the precision matrix (S.4), (c) we drew (U, Z) from their joint distribution. Based on the 1,000 samples from (U, Z) we calculated the standard deviation of U across locations, and the standard deviation of Z across locations. Figure S.3 is an equivalent to those in Figures S.1 and S.2 for correlated exposure and unmeasured covariate. Specifically, at the top of Figure S.3, we compare the standard deviation of U against the absolute value for draws from the $N(0, \sigma_{prior}^2)$ distribution, and we find that the implied confounding strength for a measured and the unmeasured covariate have similar prior distributions. At the bottom of Figure S.3, we plotted the distribution of the exposure variance against the hypothesized residual variance $\tilde{\sigma}_Z^2$, and we see that the implied prior still allow for a reasonable range of values.

Supplement F. Posterior distribution sampling scheme

We describe the MCMC updates for approximating the posterior distribution. We write $p(\theta \mid \cdot)$ to denote the posterior distribution of θ conditional on all other parameters. We use the following definitions:

- Exposure model residuals: We use \mathbf{Z}_{res} to denote the vector of length n including the exposure residuals based on the current values of the parameters γ_0, γ_C . Specifically, the i^{th} entry of \mathbf{Z}_{res} is $Z_i - \gamma_0 - \tilde{C}_i^T \gamma_C$.
- Outcome model residuals: We consider three versions of outcome model residuals, conditional on all covariates, the measured ones only, and the unmeasured covariate only. We denote them by \mathbf{Y}_{res} , \mathbf{Y}_{res}^C , and \mathbf{Y}_{res}^U with i^{th} entries

$$\begin{aligned} Y_{res,i} &= Y_i - \beta_0 - \beta_Z Z_i - \beta_{\bar{Z}} \bar{Z}_i - \tilde{C}_i \beta_C - \beta_U U_i - \beta_{\bar{U}} \bar{U}_i \\ Y_{res,i}^C &= Y_i - \beta_0 - \beta_Z Z_i - \beta_{\bar{Z}} \bar{Z}_i - \tilde{C}_i \beta_C, \quad \text{and} \\ Y_{res,i}^U &= Y_i - \beta_U U_i - \beta_{\bar{U}} \bar{U}_i, \end{aligned}$$

respectively.

- The ‘‘coefficient matrix’’ of the unmeasured covariate in the outcome model: If A_U denotes the adjacency matrix that drives the neighborhood confounder values \bar{U} in terms of U , and D_U is the corresponding degree matrix, then we have that $\bar{U} = D_U^{-1} A_U U$. Therefore, the vector U is included in the outcome model through $\beta_U U + \beta_{\bar{U}} \bar{U} = (I_n + \beta_{\bar{U}} D_U^{-1} A_U) U$, when $\beta_U = 1$. We define $M_U = I_n + \beta_{\bar{U}} D_U^{-1} A_U$ which will play a role for updating the values of the unmeasured covariate U . The matrix M_U depends on the current value of $\beta_{\bar{U}}$ so it is itself updated during the MCMC every time $\beta_{\bar{U}}$ is updated.
- The design matrices: the $n \times (p + 3)$ design matrix for the outcome model based on measured variables $\mathbf{X} = (\mathbf{1} \ \mathbf{Z} \ \bar{\mathbf{Z}} \ \mathbf{C})$, and the $n \times (p + 1)$ design matrix for the exposure model $\mathbf{X}_{-z} = (\mathbf{1} \ \mathbf{C})$.

The full list of parameters and the corresponding MCMC updates are described below. We use superscripts (r) to denote the r^{th} posterior sample of a given parameter. The updates below describe how the $(r + 1)^{th}$ sample is acquired. Most parameters are drawn using Gibbs updates, and Metropolis-Hastings is used for the spatial parameters.

- (a) $\mathbf{U}^{(r+1)}$ is drawn from its full conditional posterior distribution which is a multivariate normal with mean $\mu_{new,\mathbf{U}}$ and variance $\Sigma_{new,\mathbf{U}}$ where

$$\Sigma_{new,\mathbf{U}} = \left[G^{(r)} + (M_U^{(r)})^T M_U^{(r)} / \sigma_Y^{2(r)} \right]^{-1}, \quad \text{and}$$

$$\mu_{new,\mathbf{U}} = \Sigma_{new,\mathbf{U}} \left[(M_U^{(r)})^T \mathbf{Y}_{res}^{C,(r)} / \sigma_Y^{2(r)} - Q^{(r)} \mathbf{Z}_{res}^{(r)} \right].$$

We update the values of $\bar{\mathbf{U}}$ based on $\mathbf{U}^{(r+1)}$, and we calculate $\mathbf{Y}_{res}^{U,(r+1)}$.

- (b) We draw the intercept and the coefficients of the local exposure, neighborhood exposure, and the measured covariates in the outcome model, $(\beta_0, \beta_Z, \beta_{\bar{Z}}, \beta_C)$, from their joint full conditional distribution which is a multivariate normal with mean $\mu_{new,\beta}$ and variance $\Sigma_{new,\beta}$, where

$$\Sigma_{new,\beta} = \left[\mathbf{X}^T \mathbf{X} / \sigma_Y^{2(r)} + I_{p+3} / \sigma_{prior}^2 \right]^{-1}, \quad \text{and}$$

$$\mu_{new,\beta} = \Sigma_{new,\beta} \mathbf{X}^T \mathbf{Y}_{res}^{U,(r+1)} / \sigma_Y^{2(r)}$$

We calculate $\mathbf{Y}_{res}^{(r+1)}$ and $\mathbf{Y}_{res}^{C,(r+1)}$ based on the new β -values.

- (c) We draw the intercept and the coefficients of the measured covariates in the exposure model, (γ_0, γ_C) , from their joint full conditional distribution which is a multivariate normal with mean $\mu_{new,\gamma}$ and variance $\Sigma_{new,\gamma}$, where

$$\Sigma_{new,\gamma} = \left[\mathbf{X}_{-z}^T H^{(r)} \mathbf{X}_{-z} + I_{p+1} / \sigma_{prior}^2 \right]^{-1}, \quad \text{and}$$

$$\mu_{new,\gamma} = \Sigma_{new,\gamma} \mathbf{X}_{-z}^T \left(H^{(r)} \mathbf{Z} + (Q^{(r)})^T \mathbf{U}^{(r+1)} \right).$$

We update the exposure residuals \mathbf{Z}_{res} based on the new γ -values.

- (d) We draw the residual outcome model variance from an inverse gamma with shape parameter $\alpha_{new,Y} = \alpha_Y + n/2$, and rate parameter $\beta_{new,Y} = \beta_Y + (\mathbf{Y}_{res}^{(r+1)})^T \mathbf{Y}_{res}^{(r+1)} / 2$.

- (e) We draw the coefficient of the neighborhood unmeasured covariate from a normal distribution with mean $\mu_{new,\bar{U}}$ and variance $\sigma_{new,\bar{U}}^2$ where

$$\sigma_{new,\bar{U}}^2 = \left[(\bar{\mathbf{U}}^{(r+1)})^T \bar{\mathbf{U}}^{(r+1)} / \sigma_Y^{2(r+1)} + 1 / \sigma_{prior,\bar{U}}^2 \right]^{-1}, \quad \text{and}$$

$$\mu_{new,\bar{U}} = \sigma_{new,\bar{U}}^2 (\bar{\mathbf{U}}^{(r+1)})^T \left(\mathbf{Y}_{res}^{C,(r+1)} - \beta_U \mathbf{U}^{(r+1)} \right) / \sigma_Y^{2(r+1)}.$$

We update \mathbf{Y}_{res} and \mathbf{Y}_{res}^U based on the new value of $\beta_{\bar{U}}$.

(f) We have specified CAR structure for G, H with two parameters each $(\phi_U, \tau_U, \phi_Z, \tau_Z)$ and one parameter (ρ) for their correlation. We update all parameters using a Metropolis-Hastings step. Consider the function $\text{dexpit} : \mathbb{R} \rightarrow (-1, 1)$ with $\text{dexpit}(x) = 2/(1 + \exp(-x)) - 1$ and its inverse $\text{dexpit}^{-1} : (-1, 1) \rightarrow \mathbb{R}$ with $\text{dexpit}^{-1}(x) = \log(1 + x) - \log(1 - x)$. If $\phi_U^{(r)}, \tau_U^{(r)}, \phi_Z^{(r)}, \tau_Z^{(r)}, \rho^{(r)}$ are the current values of the parameters, we propose values $\phi_U^{prop}, \tau_U^{prop}, \phi_Z^{prop}, \tau_Z^{prop}, \rho^{prop}$ as follows:

- Draw ϵ_{ϕ_U} from $N(0, 0.35^2 s^2)$ and set $\phi_U^{prop} = \text{dexpit}(\text{dexpit}^{-1}(\phi_U^{(r)}) + \epsilon_{\phi_U})$.
- Draw ϵ_{τ_U} from $N(0, 0.2^2 s^2)$ and set $\tau_U^{prop} = \exp(\log(\tau_U^{(r)}) + \epsilon_{\tau_U})$.
- Set ϕ_Z^{prop} and τ_Z^{prop} similarly.
- Draw ϵ_{ρ} from $N(0, 0.5^2 s^2)$ and set $\rho^{prop} = \text{dexpit}(\text{dexpit}^{-1}(\rho^{(r)}) + \epsilon_{\rho})$.

Create matrices G^{prop}, H^{prop} and Q^{prop} based on the proposed values.

The acceptance probability for the joint move is given by the ratio of the posterior probabilities of the proposed values versus the current values:

$$\frac{p(\phi_U^{prop}, \tau_U^{prop}, \phi_Z^{prop}, \tau_Z^{prop}, \rho^{prop} \mid \cdot)}{p(\phi_U^{(r)}, \tau_U^{(r)}, \phi_Z^{(r)}, \tau_Z^{(r)}, \rho^{(r)} \mid \cdot)},$$

where $p(\phi_U, \tau_U, \phi_Z, \tau_Z, \rho \mid \cdot)$ is proportional to the likelihood of (8) based on the current values $\gamma_0^{(r+1)}, \gamma_C^{(r+1)}$ and $\mathbf{U}^{(r+1)}$ times the prior distribution for these spatial parameters evaluated at the proposed (numerator) or current (denominator) values. If $\phi_Z^{prop} > \phi_U^{prop}$, these values do not satisfy the prior constraint, and the proposal will be rejected.

Supplement G. Simulation results on pairs of data

For pairs of observations, we specified the adjacency matrix as block diagonal, where each block was the 2×2 matrix $\begin{pmatrix} 0 & 1 \\ 1 & 0 \end{pmatrix}$. For the simulations on network data in Section 5, the network has median degree 2, and we set $\tau_U^2 = \tau_Z^2 = 1$. For the pair data, for which median node degree is equal to 1, we set $\tau_U^2 = \tau_Z^2 = 2$, in order to ensure similar marginal variability in the exposure and the unmeasured confounder in the network and paired data settings

Table S.3 shows the simulation results for pairs of data with 100, 175, and 250 pairs of observations (total number of observations 200, 350, and 500). We present bias, root mean squared error and coverage of 95% intervals for the OLS estimator and for our approach, for the local and the interference effects. These results mirror the results for network data shown in Table 1, and the conclusions from the two settings are unaltered.

Table S.3: Simulation results for paired data. Results show the bias, root mean squared error and coverage of 95% intervals for the local and interference effects based on the OLS estimator and our approach.

True model & sample size	Local effect						Interference effect						
	OLS			Our approach			OLS			Our approach			
	Bias	RMSE	Cover	Bias	RMSE	Cover	Bias	RMSE	Cover	Bias	RMSE	Cover	
$\beta_Z = 0$ and $\beta_{\bar{U}} = 0$													
3a	200	0.660	0.669	0	-0.037	0.300	95.6	0.151	0.172	55	0.017	0.107	93.6
	350	0.660	0.664	0	-0.019	0.236	98.1	0.144	0.155	38	0.009	0.077	95.4
	500	0.670	0.673	0	-0.058	0.238	94	0.147	0.155	17.7	0.009	0.064	97.9
$\beta_Z = 0$													
3b	200	0.923	0.932	0	-0.154	0.296	95.2	0.269	0.285	21.7	0.021	0.124	96.1
	350	0.920	0.925	0	-0.158	0.260	94.9	0.265	0.273	2.3	0.008	0.096	96.5
	500	0.933	0.936	0	-0.154	0.241	92.6	0.270	0.276	0.7	0.012	0.080	96
$\beta_{UZ} = 0$ and $\beta_U = \beta_{\bar{U}} = 0$													
3c	200	0.004	0.095	96	-0.027	0.125	99.1	0.005	0.064	94.7	0.003	0.064	96.5
	350	-0.003	0.069	95.7	-0.017	0.107	99.6	-0.004	0.047	95.3	-0.006	0.048	98.4
	500	0.000	0.065	92.3	-0.030	0.108	99.6	0.001	0.041	94.3	0.003	0.043	95.1
$\beta_U = 0$ and $\beta_{\bar{U}} = 0$													
3d	200	0.002	0.079	95.3	-0.026	0.122	98.3	0.005	0.061	94.7	-0.001	0.063	96.6
	350	-0.002	0.057	95.7	-0.032	0.112	98	-0.003	0.044	95.7	-0.011	0.052	95
	500	0.000	0.054	91.7	-0.063	0.181	88.6	0.001	0.039	93.7	-0.001	0.048	92.4
$\beta_{\bar{U}} = 0$													
3e	200	0.660	0.669	0	0.020	0.262	96.9	0.151	0.172	55	0.017	0.107	94.4
	350	0.660	0.664	0	0.019	0.212	96.6	0.144	0.155	38	0.009	0.078	96.6
	500	0.670	0.673	0	0.033	0.186	96.4	0.147	0.155	17.7	0.012	0.063	96.8
3f	200	0.923	0.932	0	-0.111	0.266	96.9	0.269	0.285	21.7	0.014	0.124	95.7
	350	0.920	0.925	0	-0.113	0.225	95.7	0.265	0.273	2.3	0.004	0.095	96
	500	0.933	0.936	0	-0.107	0.199	95.3	0.270	0.276	0.7	0.009	0.078	96.7

Supplement H. Additional study information

H.1 The data set

We assemble a data set on power plant emissions and characteristics, population demographics, weather, and information on cardiovascular mortality among the elderly, measured at the level of US counties. We briefly describe the data set here.

We acquire power plant emissions and characteristics for 2004 based on the publicly available data from [Papadogeorgou et al. \[2019\]](#). Power plant information includes the number of power plant units in the facility, whether the plant uses mostly natural gas or coal (an important predictor of SO_2 emissions), its total emissions, heat input and operating capacity, whether it has a technology installed for oxides of nitrogen control, and whether the plant participated in Phase II of the Acid Rain Program. Our data set includes 906 power plant facilities in 596 counties. We aggregate power plant information at the county level, and define the total SO_2 emissions from all power plants in the county as the exposure of interest. We consider first and second degree county-level adjacency matrices. The first degree adjacency matrix A^1 has (i, j) entry equal to 1 if counties i and j share a border, and 0 otherwise. Instead the (i, j) entry of the second degree adjacency matrix A^2 is equal to 1 if i and j share a border or a first-degree neighbor. Considering the size of counties in the US and the potential long-distance pollution transport, we define the neighborhood exposure \bar{Z} using the second degree adjacency matrix A^2 , allowing neighbors of neighbors to contribute to potential interference effects.

We considered demographic information as potential confounders. Specifically, we consider population characteristics such as percentages of urbanicity, of white and hispanic population, of population with at least a high school diploma, of population that lives below the poverty limit, of female

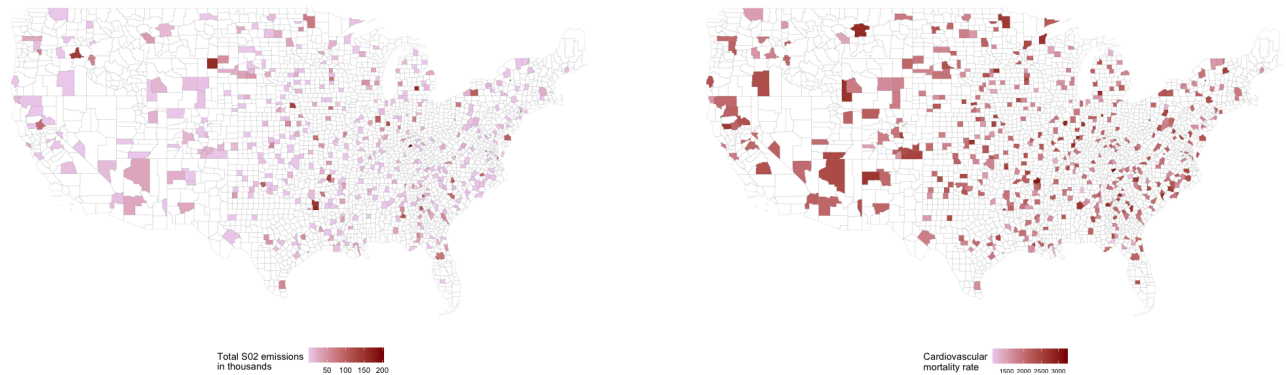


Figure S.4: County-level exposure (left) and outcome (right) on the 445 counties in our data set.

population, of population having lived in the area for less than 5 years, of housing units that are occupied, and population per square mile from the 2000 Census, and also county-level smoking rates acquired using the CDC Behavioral Risk Factor Surveillance System data.

We downloaded county level weather data for 2004 from the National Oceanic and Atmospheric Administration's (NOAA) data base, available at <ftp://ftp.ncdc.noaa.gov/pub/data/cirs/climdiv/>. Specifically, we acquired data for each county describing the maximum, minimum and average temperature, and total precipitation for each month in 2004. We aggregated the data across the twelve months by considering the total yearly precipitation, the second most extreme of the monthly maximum and minimum temperatures, the average maximum and minimum temperatures, and the average, maximum and minimum of the average monthly temperatures. After examining the correlation matrix, we deduced that many covariates were highly correlated, and used only the three mentioned above (total precipitation, second maximum and minimum temperatures).

We acquire health information from the United States Centers for Disease Control and Prevention (CDC) WONDER query system. We consider deaths due to the diseases of the circulatory system (I-00 to I-99 codes) among population aged 65 years or older, and define the outcome of interest as the number of deaths per 100,000 residents in 2005.

We merge power plant, weather, health and demographic information. We only keep counties with at least one neighbor with SO₂ emissions from power plants, since the interference effect of changing neighborhood exposure would not be well-defined for a county without neighbors with emissions. The final data set includes 445 counties in 44 US states, illustrated in Figure S.4.

H.2 Analysis including weather variables

We found that OLS estimates for the local and interference effect are comparable when weather variables are included or not (Figure S.5). Therefore, we have focused in our main text on the analyses excluding weather variables.

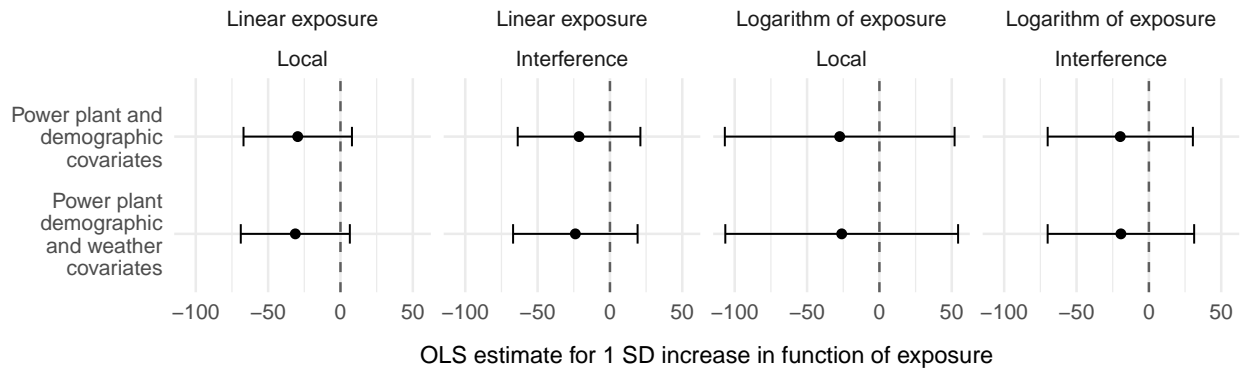


Figure S.5: OLS estimates for the local and interference effect of exposure or the logarithmic transformation for exposure when adjusting for local and neighborhood values of power plant and demographic characteristics only, or also including weather information